Electronic Supplementary Material (ESI) for Journal of Materials Chemistry
This journal is © The Royal Society of Chemistry 2012

Supporting Information

Colour Tuning from Green to Red by Substituent Effects in Phosphorescent Tris-Cyclometalated Iridium(III) Complexes of Carbazole-Based Ligands: Synthetic, Photophysical, Computational and High Efficiency OLED Studies

Mustafa Tavasli,[a] Tom N. Moore,[b] Yonghao Zheng,[b] Martin R. Bryce,*[,b] Mark A. Fox,[b] Gareth C. Griffiths,[c] Vygintas Jankus,[c] Hameed A. Al-Attar,[c] and Andrew P. Monkman[c]

[a] *Uludag Universitesi, Fen-Edebiyat Fakultesi, Kimya Bolumu, Gorukle Kampusu, 16059 Nilufer, Bursa, Turkiye*

[b] *Department of Chemistry, Durham University, Durham DH1 3LE, United Kingdom*

[c] *Department of Physics, Durham University, Durham DH1 3LE, United Kingdom*

Page

This journal is © The Royal Society of Chemistry 2012

General Details. Reactions that required an inert or dry atmosphere were performed under anhydrous argon which was dried by passage through a column of blue indicating silica gel and phosphorus pentoxide. 2-Chloro-4-methoxypyridine **7c** was synthesised according to literature methods. All reagents were of standard reagent grade and were used as supplied unless otherwise stated from Aldrich, Fluka, Lancaster, Alfa Aesar or Alpha. Where an anhydrous solvent was employed it was dried through an HPLC column on an Innovative Technology Inc. solvent purification system. Petroleum ether refers to the fraction with a boiling point of 40-60 ^{o}C. Column chromatography was carried out using silica gel (40-60 μm). Thin layer chromatography was carried out using Polygram SilG/UV F_{254} TLC plates, with visualisation using ultraviolet light (254 or 365 nm). ^{1}H NMR spectra were recorded on either a Bruker Avance 400 at 400MHz or a Varian Inova 500 instrument at 500MHz. ^{13}C NMR spectra were recorded on the above spectrometers using broad-band decoupling at 100 MHz and 125 MHz, respectively. Chemical shifts are reported in ppm downfield of tetramethylsilane (TMS), using TMS or the residual non-deuterated solvent as the internal reference. Electrospray (ES^{+}) mass spectra were recorded on a Micromass LCT mass spectrometer. Matrix assisted laser desorption ionisation time of flight (MALDI-ToF) mass spectra were recorded on an Applied Biosystems Voyager-DE STR mass spectrometer. GC-MS mass spectra were recorded on a Thermo-Finnigan Trace mass spectrometer. Melting points were determined using a Stuart Scientific SMP3 melting point apparatus and are uncorrected. Elemental analyses were obtained on an Exeter Analytical Inc. CE-440 elemental analyser.

Synthetic Details.

Preparation of the Ligands

General procedure: An argon-filled flask was charged with degassed solutions of Cz-3'-yl or -2'-yl-boronic acids (**5** and **6**) in toluene (40 mL for series 1 or 150 mL for series 2) and aqueous Na_2CO_3 solution. To this, a catalytic amount of bis(triphenylphosphine)palladium(II) dichloride, $(PPh_3)_2PdCl_2$ (for series 1) or tetrakis(triphenylphosphine)palladium(0), $(PPh_3)_4Pd$ (for series 2) and 2-halo-4/5-substituted pyridine, 2-X-4/5-R-Py (**7b-e**) were added and the whole mixture was heated at 90 ^{o}C for 65 h (for series 1) or 96 h (for series 2). Upon cooling, the mixture was diluted with distilled H_2O and the organic products were extracted into CH_2Cl_2 (4x30 mL). The combined extracts were dried over $MgSO_4$ and then concentrated under reduced pressure to give a crude product. Purification (by column chromatography over silica-gel, or distillation using a Kugelrohr, or crystallisation) afforded the title ligands.

This journal is © The Royal Society of Chemistry 2012

2-(*N*-*n*-hexylcarbazol-3'-yl)-4-trifluoromethylpyridine 3b: A mixture of Cz-3'yl-boronic acid **5** (0.50 g, 1.69 mmol), aq. Na_2CO_3 (2 M, 9.7 mL, 19.38 mmol), $(PPh_3)_2PdCl_2$ (0.08 g, 0.11 mmol) and 2-Cl-4-CF_3-Py **7b** (0.29 g, 1.61 mmol) afforded **3b** (0.42 g, 66%) as a light yellow solid. R_f (hexane:CH_2Cl_2, 1:1 v/v) = 0.14; mp 74-75 ^oC; ^1H NMR (400 MHz, $CDCl_3$) δ_H 8.88 (1H, d, *J* 5.0), 8.81 (1H, d, *J* 1.7), 8.20 (1H, d, *J* 7.9), 8.17 (1H, dd, *J* 8.4, 1.8) 8.06 (1H, s), 7.51-7.48 (2H, m), 7.45-7.05 (2H, m), 7.28 (1H, td, *J* 7.4, 1.1), 4.34 (2H, t, *J* 7.3, NCH_2), 1.96-1.88 (2H, m, NCH_2CH_2), 1.44-1.33 (6H, m), 0.86 (3H, t, *J* 6.8, CH_3); ^{13}C NMR (101 MHz, $CDCl_3$) δ_C 147.05, 142.30, 141.87, 141.28, 126.38, 125.05, 123.72, 123.29, 123.22, 120.92, 119.71, 119.67, 109.32, 109.26, 43.54, 31.13, 29.17, 27.18, 22.74, 14.20; GC-MS (EI) *m/z* = 325 (M^+ - C_5H_{11}, 100%), 396 (M^+, 71); Anal. Calcd. for $C_{24}H_{23}F_3N_2$: C, 72.7; H, 5.85; N, 7.1. Found: C, 72.5; H, 5.9; N, 7.0.

2-(*N*-*n*-hexylcarbazol-3'-yl)-4-methoxypyridine 3c: A mixture of Cz-3'-ylboronic acid **5** (0.50 g, 1.69 mmol), aq. Na_2CO_3 (2 M, 9.7 mL, 19.38 mmol), $(PPh_3)_2PdCl_2$ (0.08 g, 0.11 mmol) and 2-Cl-4-MeO-Py **7c**[1] (0.23 g, 1.61 mmol) afforded **3c** (0.21 g, 36%) as a light orange oil. R_f (CH_2Cl_2:EtOAc, 9:1 v/v) = 0.35; ^1H NMR (400 MHz, $CDCl_3$) δ_H 8.76 (1H, dd, *J* 1.8, 0.5), 8.58 (1H, d, *J* 5.7), 8.21 (1H, d, *J* 7.5), 8.12 (1H, dd, *J* 8.6, 1.8), 7.54-7.42 (3H, m), 7.38 (1H, d, *J* 2.2), 7.31-7.25 (1H, m), 6.79 (1H, dd, *J* 5.7, 2.4), 4.35 (2H, t, *J* 7.2, NCH_2), 3.97 (3H, s, OCH_3), 1.95-1.88 (2H, m, NCH_2CH_2), 1.47-1.24 (6H, m), 0.89 (3 H, t, *J* 7.1, CH_3); ^{13}C NMR (101 MHz, $CDCl_3$) δ_C 166.64, 160.32, 150.97, 141.35, 141.17, 130.60, 126.02, 125.04, 123.41, 120.83, 119.38, 119.30, 109.07, 108.93, 107.57, 106.51, 55.36, 43.45, 31.78, 29.17, 27.17, 22.74, 14.20; MS (ES^+) *m/z* = 359 (M^+, 100%). MS (ASAP+) Calcd. for [$C_{24}H_{26}N_2O$ + H^+]: 359.2123. Found: 359.21171.

2-(*N*-*n*-hexylcarbazol-3'-yl)-5-trifluoromethylpyridine 3d: A mixture of Cz-3'-ylboronic acid **5** (0.56 g, 1.90 mmol), aq. Na_2CO_3 (2 M, 9.7 mL, 19.38 mmol), $(PPh_3)_2PdCl_2$ (0.08 g, 0.11 mmol) and 2-Cl-5-CF_3-Py **7d** (0.86 g, 4.75 mmol) afforded **3d** (0.53 g, 71%) as an off white solid. R_f (petroleum ether:CH_2Cl_2, 2:1 v/v) = 0.23; mp 88-89 ^oC; ^1H NMR (500 MHz, C_6D_6) δ_H 8.98 (1H, s), 8.93 (1H, d, *J* 1.6), 8.39 (1H, dd, *J* 8.6, 1.8), 8.11 (1H, d, *J* 7.7), 7.44-7.37 (2H, m), 7.30 (1H, d, *J* 8.4), 7.26 (1H, t, *J* 7.1), 7.22 (1H, d, *J* 8.6), 7.16 (1H, t, *J* 4.0), 3.76 (2H, t, *J* 7.2, NCH_2), 1.53-1.44 (2H, m, NCH_2CH_2), 1.14-0.98 (6H, m), 0.79 (3H, t, *J* 7.1, CH_3); ^{13}C NMR (126 MHz, C_6D_6) δ_C 161.88, 147.05, 142.44, 141.83, 133.88, 129.70, 126.77, 125.98, 124.21, 124.06, 123.96, 121.36, 120.53, 120.26, 119.37, 109.72, 109.58, 43.39, 32.10, 29.40, 27.44, 23.15, 14.52; GC-MS (EI) *m/z* = 325 (M^+ - C_5H_{11}, 100%), 396 (M^+, 71); Anal. Calcd. for $C_{24}H_{23}F_3N_2$: C, 72.7; H, 5.85; N, 7.1. Found: C, 72.8; H, 5.9; N, 7.0.

This journal is © The Royal Society of Chemistry 2012

2-(*N*-*n*-hexylcarbazol-3'-yl)-5-methoxypyridine 3e: A mixture of Cz-3'-ylboronic acid **5** (0.51 g, 1.73 mmol), aq. Na_2CO_3 (2 M, 9.7 mL, 19.38 mmol), $(PPh_3)_2PdCl_2$ (0.08 g, 0.11 mmol) and 2-Br-5-MeO-Py **7e** (0.80 g, 4.23 mmol), upon purification over silica-gel and followed by Kugelrohr distillation, afforded **3e** (0.27 g, 44%) as a light orange oil. R_f (CH_2Cl_2:EtOAc, 20:1 v/v) = 0.41; ^{1}H NMR (400 MHz, $CDCl_3$) δ_H 8.74 (1H, s), 8.46 (1H, d, *J* 3.0), 8.21 (1H, d, *J* 7.8), 8.05 (1H, dd, *J* 8.6, 1.1), 7.68 (1H, d, *J* 8.7), 7.48 (1H, t, *J* 7.6), 7.41-7.38 (2H, m), 7.28 (1H, t, *J* 7.4), 7.18 (1H, dd, *J* 8.7, 2.9), 4.22 (2H, t, *J* 7.2, NCH_2), 3.80 (3H, s, OCH_3), 1.88–1.77 (2H, m, NCH_2CH_2), 1.32-1.25 (6H, m), 0.88 (3H, t, *J* 6.9, CH_3); ^{13}C NMR (101 MHz, $CDCl_3$) δ_C 154.27, 151.10, 140.98, 140.64, 136.86, 130.23, 125.78, 124.45, 123.31, 123.24, 121.48, 120.42, 119.02, 118.43, 108.88, 108.82, 55.59, 43.13, 31.60, 28.97, 26.97, 22.57, 14.05; MS (ES^+) *m/z* = 359 (M^+, 100%). Anal. Calcd. for $C_{24}H_{26}N_2O$: C, 80.4; H, 7.3; N, 7.8. Found: C, 80.1; H, 7.4; N, 7.5.

2-(*N*-*n*-hexylcarbazol-2'-yl)-4-trifluoromethylpyridine 4b: A mixture of Cz-2'-ylboronic acid **6** (1.00.g, 3.39 mmol), aq. Na_2CO_3 (2 M, 4.13 g, 38.99 mmol), $Pd(PPh_3)_4$ (0.25 g, 0.22 mmol) and 2-Cl-4-CF_3-Py **7b** (0.59 g, 3.24 mmol) afforded **4b** (0.78 g, 61%) as a white powder. R_f (petroleum ether:CH_2Cl_2, 1:1 v/v) = 0.35; mp 120-121 ^{o}C; ^{1}H NMR (400 MHz, $CDCl_3$) δ_H 8.89 (1H, d, *J* 5.0), 8.20-8.10 (3H, m), 8.05 (1H, s), 7.83 (1H, dd, *J* 8.2, 1.5), 7.49 (1H, td, *J* 8.2, 1.2), 7.45-7.41 (2H, m), 7.27-7.22 (1H, m), 4.38 (2H, t, *J* 7.3, NCH_2), 1.98-1.83 (2H, m, NCH_2CH_2), 1.46-1.21 (6H, m), 0.85 (3H, t, *J* 7.1, CH_3); ^{13}C NMR (101 MHz, $CDCl_3$) δ_C 159.83, 150.79, 141.67, 141.13, 139.31, 135.69, 126.53, 124.48, 123.30, 122.59, 120.99, 120.91, 119.34, 118.00, 117.36, 116.54, 109.16, 107.71, 43.38, 31.80, 29.23, 27.18, 22.77, 14.21; GC-MS (EI) *m/z* = 325 (M^+ - C_5H_{11}, 100%), 396 (M^+, 58). Anal. Calcd. for $C_{24}H_{23}F_3N_2$: C, 72.7; H, 5.9; N, 7.1. Found: C, 72.7; H, 5.9; N, 7.1.

2-(*N*-*n*-hexylcarbazol-2'-yl)-5-trifluoromethylpyridine 4d: A mixture of Cz-2'-ylboronic acid **6** (1.00 g, 3.39 mmol), aq. Na_2CO_3 (2 M, 4.13 g, 38.99 mmol), $Pd(PPh_3)_4$ (0.25 g, 0.22 mmol), 2-Cl-5-CF_3-Py **7d** (0.59 g, 3.22 mmol) afforded the **4d** (0.70 g, 55%) as an off-white/yellow solid. R_f (petroleum ether:CH_2Cl_2, 1:1 v/v) = 0.43; mp 112-113 ^{o}C; ^{1}H NMR (400 MHz, $CDCl_3$) δ_H 8.97 (1H, s), 8.18-8.16 (2H, m), 8.12 (1H, d, *J* 7.7), 8.02-7.94 (2H, m), 7.82 (1H, dd, *J* 8.3, 1.4), 7.49 (1H, dt, *J* 8.2, 1.2), 7.42 (1H, d, *J* 8.2), 7.28-7.21 (1H, m), 4.38 (2H, t, *J* 7.3, NCH_2), 1.96-1.85 (2H, m, NCH_2CH_2), 1.46-1.23 (6H, m), 0.84 (3H, t, *J* 7.1, CH_3); ^{13}C NMR (101 MHz, $CDCl_3$) δ_C 161.67, 146.78, 141.71, 141.10, 135.52, 134.05, 126.61, 124.66, 124.65, 124.12, 122.57, 121.01, 120.87, 120.42, 119.36, 118.17, 109.18, 108.01, 43.40, 31.81, 29.24, 27.19,

This journal is © The Royal Society of Chemistry 2012

22.77, 14.22; GC-MS (EI) *m/z* = 55 (100%), 146 (M^+ - $C_{18}H_{20}N$, 46), 325 (M^+ - C_5H_{11}, 29), 396 (M^+, 8); Anal. Calcd. for $C_{24}H_{23}F_3N_2$: C, 72.7; H, 5.9; N, 7.1. Found: C, 72.7; H, 5.8; N, 7.0.

2-(*N*-*n*-hexylcarbazol-2'-yl)-5-methoxypyridine 4e: A mixture of Cz-2'-ylboronic acid **6** (1.00 g, 3.39 mmol), aq. Na_2CO_3 (2 M, 4.13 g, 38.99 mmol), $Pd(PPh_3)_4$ (0.25 g, 0.22 mmol) and 2-Br-5-MeO-Py **7e** (0.60 g, 3.17 mmol) afforded **4e** (0.52 g, 46%) as a white solid. R_f (CH_2Cl_2) = 0.23; mp 117-118 °C; ^{1}H NMR (400 MHz, $CDCl_3$) δ_H 8.43 (1H, d, *J* 2.9), 8.12 (1H, dd, *J* 0.5, 8.1), 8.09 (1H, d, *J* 7.5), 8.04 (1H, s), 7.79 (1H, d, *J* 8.7), 7.73 (1H, dd, *J* 8.2, 1.5), 7.45 (1H, td, *J* 8.1, 1.2), 7.40 (1H, d, *J* 8.1), 7.30 (1H, dd, *J* 8.7, 3.0), 7.21 (1H, td, *J* 7.9, 1.1), 4.36 (2H, t, *J* 7.4, NCH_2), 3.91 (3H, s, OCH_3), 1.94-1.84 (2H, m, NCH_2CH_2), 1.46-1.21 (6H, m), 0.84 (3H, t, *J* 7.1, CH_3); ^{13}C NMR (101 MHz, $CDCl_3$) δ_C 155.00, 151.32, 141.50, 141.34, 137.33, 137.14, 126.02, 123.19, 122.93, 121.69, 120.76, 120.70, 119.14, 117.77, 109.06, 106.99, 100.29, 56.03, 43.41, 31.91, 29.30, 27.28, 22.88, 14.33; GC-MS (EI) *m/z* = 287 (M^+ - C_5H_{11}, 100%), 358 (M^+, 89); Anal. Calcd. for $C_{24}H_{26}N_2O$: C, 80.3; H, 7.3; N, 7.8. Found: C, 80.3; H, 7.3; N, 7.9.

Preparation of the Complexes

Complexes 1a and **2a** were synthesized as described previously.[2]

Complex 1b: *Route A.* A mixture of **3b** (0.40 g, 1.01 mmol), $Ir(acac)_3$ (0.12 g, 0.25 mmol) and glycerol (15 mL) afforded **1b** (0.02 g, 2%) as a bright orange powder. R_f (hexane:CH_2Cl_2, 1:1 v/v) = 0.71; mp 328 °C; ^{1}H NMR (500 MHz, CD_2Cl_2) δ_H 8.53 (3H, s), 8.30 (3H, s), 8.06 (3H, d, *J* 7.6), 7.91 (3H, d, *J* 5.8), 7.34 (3H, t, *J* 7.7), 7.20 (3H, d, *J* 8.2), 7.15 (3H, t, *J* 7.5), 7.06 (3H, dd, *J* 5.8, 1.6), 6.73 (3H, s), 3.78-3.63 (6H, m, NCH_2), 1.41-1.36 (6H, m, NCH_2CH_2), 0.93-0.84 (12H, m), 0.83-0.76 (6H, t, *J* 16.6), 0.65 (9H, t, *J* 6.8); ^{13}C NMR (126 MHz, CD_2Cl_2) δ_C 168.97, 160.07, 148.89, 144.67, 140.75, 138.33, 134.93, 124.95, 124.60, 123.60, 119.45, 118.19, 117.88, 116.95, 116.06, 114.88, 109.10, 43.17, 31.78, 28.86, 27.22, 22.80, 14.17; MS (MALDI-TOF) *m/z* = 1379 (M^+, 100%). Anal. Calcd. for $C_{72}H_{66}F_9IrN_6$: C, 62.73; H, 4.83; N, 6.10. Found: C, 62.60; H, 4.95; N, 5.94.

Route B. A mixture of the ligand **3b** (0.23 g, 0.58 mmol), iridium chloride (0.09 g, 0.25 mmol) and 2-ethoxyethanol: water (10 mL, 3:1 v/v) was stirred at 120 °C for 15 h to give a precipitate of the intermediate μ-chloro-bridged dimer which was collected and dried as an orange solid (0.24 g). A mixture of the dimer (0.24 g), **3b** (0.20 g, 0.60 mmol), ethylene glycol (10 mL), acetylacetone (0.1 mL) and NEt_3 (0.1 mL) was stirred at 190 °C for 1 h. The precipitate was collected and purified by column chromatography (silica, dichloromethane:hexane, 4:6 v/v) to yield complex **1b** (0.16 g, 51%) identical with the sample above.

This journal is © The Royal Society of Chemistry 2012

Complex 1c: *Route B*. A mixture of the **3c** (0.67 g, 1.9 mmol), iridium chloride (0.32 g, 0.89 mmol) and 2-ethoxyethanol: water (10 mL, 3:1 v/v) gave the intermediate μ-chloro-bridged dimer as a yellow solid (0.38 g). A mixture of **3c** (0.08 g, 0.23 mmol), the dimer (0.11 g, 0.06 mmol) in ethylene glycol (10 mL), acetylacetone (0.1 mL) and NEt_3 (0.1 mL) gave a precipitate which was purified by column chromatography (SiO_2, dichloromethane:hexane, 4:6 v/v) yielding complex **1c** (0.10 g, 70%) as a yellow solid; mp 309 ^oC; δ_H (500 MHz, acetone-d_6) 8.63 (3H, s), 8.05 (3H, d, *J* 7.6), 7.78 (3H, d, *J* 2.6), 7.66 (3H, t, *J* 6.6), 7.31 – 7.23 (6H, m), 7.07 (3H, ddd, *J* 13.0, 7.5, 4.5), 6.94 (3H, s), 6.64 (3H, dd, *J* 6.4, 2.6), 3.98 (9H, s), 3.86 – 3.71 (6H, m), 1.55 – 1.26 (12H, m), 1.02 – 0.81 (12H, m), 0.66 (9H, m). ^{13}C NMR (126 MHz, acetone-d_6) 168.98, 166.39, 162.14, 148.36, 143.75, 140.25, 137.26, 124.87, 123.75, 118.75, 118.40, 116.92, 116.30, 115.51, 108.51, 108.42, 103.02, 55.31, 42.54, 31.37, 28.56, 26.77, 22.36, 13.58; MS (MALDI-TOF): *m/z* 1264.4 (M^+, 100%). HRMS (AP^+), [$C_{72}H_{75}{}^{193}IrN_6O_3$]: Calcd. 1264.5530. Found: 1264.5540. Anal. Anal. Calcd. for $C_{72}H_{75}{}^{193}IrN_6O_3$: C, 68.38; H, 5.98; N, 6.65. Found: C, 68.15; H, 5.88; N, 6.83.

Complex 1d: *Route A*. A mixture of **3d** (0.47 g, 1.19 mmol) and $Ir(acac)_3$ (0.12 g, 0.25 mmol) and glycerol (15 mL) afforded **1d** (0.08 g, 8%) as a light yellow powder. R_f (hexane:CH_2Cl_2, 1:1 v/v) = 0.71; mp 333 ^oC; ^1H NMR (400 MHz, $CDCl_3$) δ_H 8.47 (3H, s), 8.13 (3H, d, *J* 8.6), 8.03 (3H, d, *J* 7.6), 7.84-7.74 (6H, m), 7.32 (3H, t, *J* 7.5), 7.17-7.12 (6H, m), 6.74 (3H, s), 3.76-3.63 (6H, m, NCH_2), 1.42-1.37 (6H, m, NCH_2CH_2), 0.88-0.75 (18H, m), 0.63 (9H, t, *J* 6.5, CH_3); ^{13}C NMR (101 MHz, $CDCl_3$) δ_C 170.66, 160.35, 144.60, 140.52, 134.30, 133.35, 129.02, 124.73, 124.38, 123.82, 123.49, 121.94, 119.19, 118.27, 118.24, 118.12, 115.69, 108.71, 42.91, 31.45, 28.53, 26.86, 22.44, 14.10; MS (MALDI-TOF) *m/z* = 1379 (M^+, 100%). MS (ASAP) Calcd. for [$C_{72}H_{66}F_9{}^{193}IrN_6$]: 1378.4836. Found: 1378.4869. Anal. Calcd. for $C_{72}H_{66}F_9IrN_6$: C, 62.73; H, 4.83; N, 6.10. Found: C, 62.99; H, 4.99; N, 6.20.

Complex 1e: *Route A*. A mixture of **3e** (0.27 g, 0.75 mmol) $Ir(acac)_3$ (0.11 g, 0.21 mmol) and glycerol (15 mL) afforded **1e** (0.07 g, 8%) as a bright yellow/green powder. R_f (CH_2Cl_2) = 0.72; mp 355 ^oC; ^1H NMR (500 MHz, CD_2Cl_2) δ_H 8.33 (3H, s), 8.03-8.01 (6H, m), 7.44 (3H, d, *J* 2.7), 7.33-7.25 (6H, m), 7.16 (3H, d, *J* 8.1), 7.09 (3H, t, *J* 7.4), 6.79 (3H, s), 3.75-3.68 (6H, m, NCH_2), 3.66 (9H, d, *J* 9.6, OCH_3), 1.42-1.36 (6H, m, NCH_2CH_2), 0.94-0.85 (12H, m), 0.84-0.77 (6H, m), 0.65 (9H, t, *J* 6.8, CH_3); ^{13}C NMR (126 MHz, CD_2Cl_2) δ_C 160.75, 158.99, 154.91, 143.44, 140.46, 136.87, 134.89, 124.86, 124.05, 121.99, 119.11, 119.08, 118.63, 117.18, 115.88, 115.35, 108.70, 56.12, 43.10, 31.81, 28.90, 27.21, 22.81, 14.26; MS (MALDI-TOF) *m/z* = 1265

(M^+, 100%). MS ($ASAP^+$) Calcd. for [$C_{72}H_{75}{}^{193}IrN_6O_3$]: 1264.5530. Found: 1264.5540. Anal. Anal. Calcd. for $C_{72}H_{75}{}^{193}IrN_6O_3$: C, 68.38; H, 5.98; N, 6.65. Found: C, 68.55; H, 6.00; N, 6.60.

Complex 2b: *Route A*. A mixture of **4b** (0. 41g, 1.02 mmol), $Ir(acac)_3$ (0.15 g, 0.31 mmol) and glycerol (15 mL) afforded **2b** (0.03 g, 2%) as a dark red powder. R_f (petroleum ether:CH_2Cl_2, 1:1 v/v) = 0.64; ^1H NMR (500 MHz, CD_2Cl_2) δ_H 8.31 (3H, s), 7.88-7.89 (6H, m), 7.49 (3H, d, *J* 7.9), 7.40 (3H, s), 7.31-7.29 (6H, m), 7.08 (3H, d, *J* 5.5), 6.87-6.84 (3H, m), 4.34 (6H, t, *J* 7.1, NCH_2), 1.97-1.88 (6H, m, NCH_2CH_2), 1.49-1.22 (18H, m), 0.88 (9H, t, *J* 7.1, CH_3); ^{13}C NMR (126 MHz, CD_2Cl_2) δ_C 169.34, 148.87, 147.93, 142.17, 140.61, 138.12, 137.72, 127.84, 124.67, 126.30, 123.59, 122.38, 121.43, 118.33, 118.12, 115.68, 108.88, 106.19, 43.46, 32.26, 29.50, 27.54, 23.17, 14.39; MS (MALDI-TOF) *m/z* = 1379 (M^+, 100%); Anal. Calcd. for $C_{72}H_{66}F_9{}^{193}IrN_6$: C, 62.73; H, 4.83; N, 6.10. Found: C, 63.35; H, 5.20; N, 5.65.

Complex 2d: *Route A*. A mixture of **4d** (0.41 g, 1.03 mmol), $Ir(acac)_3$ (0.14 g, 0.29 mmol) and glycerol (15 mL) afforded **2d** (0.01 g, 1%) as a dark red powder. R_f (petroleum ether:CH_2Cl_2, 1:1 v/v) = 0.74; mp 371 ^oC; ^1H NMR (500 MHz, CD_2Cl_2) δ_H 8.25 (3H, d, *J* 9.3), 7.90-7.86 (9H, m), 7.50 (3H, d, *J* 7.8), 7.43 (3H, s), 7.34-7.27 (6H, m), 6.87-6.84 (3H, m,), 4.33 (6H, t, *J* 7.4, NCH_2), 1.98-1.87 (6H, m), 1.46-1.29 (18H, m), 0.88 (9H, t, *J* 7.2, CH_3); ^{13}C NMR (126 MHz, CD_2Cl_2) δ_C 171.50, 148.54, 144.74, 142.29, 140.32, 137.75, 133.84, 128.01, 127.76, 126.45, 124.72, 123.64, 122.33, 121.53, 119.55, 118.34, 108.77, 107.01, 43.50, 32.23, 29.48, 27.59, 23.18, 14.38; MS (MALDI-TOF) *m/z* = 1378 (M^+, 100%). MS ($ASAP^+$) Calcd. for [$C_{72}H_{66}F_9{}^{193}IrN_6$]: 1378.4836. Found: 1378.4869.

Complex 2e: *Route A*. A mixture of **4e** (0.30 g, 0.84 mmol), $Ir(acac)_3$ (0.13 g, 0.26 mmol) and glycerol (15 mL) afforded **2e** (0.08 g, 8%) as a bright orange powder. R_f (petroleum ether:CH_2Cl_2, 1:1 v/v) = 0.78; mp 365 ^oC; ^1H NMR (500 MHz, CD_2Cl_2) δ_H 8.04 (3H, d, *J* 9.1), 7.69 (3H, s), 7.49 (3H, d, *J* 7.8), 7.37 (3H, d, *J* 2.7), 7.28-7.22 (12H, m), 6.82-6.76 (3H, m), 4.42-4.33 (6H, m, NCH_2), 3.66 (9H, s, OCH_3), 1.96-1.88 (6H, m, NCH_2CH_2), 1.47-1.42 (6H, m), 1.41-1.25 (12H, m), 0.88 (9H, t, *J* 7.2, CH_3); ^{13}C NMR (126 MHz, CD_2Cl_2) δ_C 160.37, 155.64, 145.69, 143.09, 141.18, 138.21, 135.45, 127.83, 125.24, 125.04, 122.96, 121.09, 121.00, 119.99, 117.99, 108.58, 103.86, 56.07, 43.15, 32.28, 29.89, 27.60, 23.19, 14.42; MS (MALDI-TOF) *m/z* = 1265 (M^+, 100%); Anal. Calcd. for $C_{72}H_{75}{}^{193}IrN_6O_3$: C, 68.38; H, 5.98; N, 6.65. Found: C, 68.3; H, 6.0; N, 6.6.

This journal is © The Royal Society of Chemistry 2012

NMR Spectra of the New Complexes

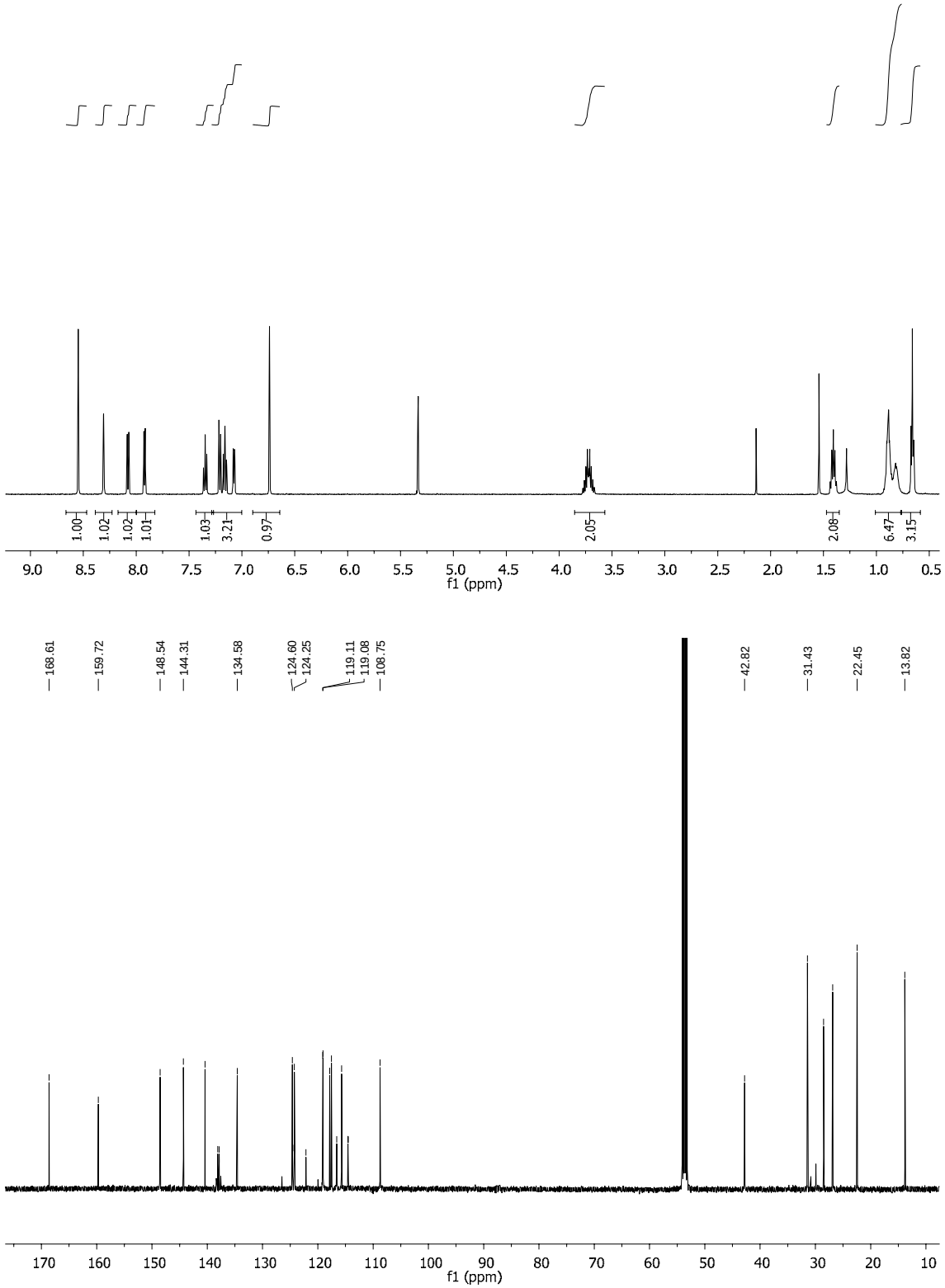

Figure S1. ^{1}H and ^{13}C NMR spectra of **1b** in CD_2Cl_2.

This journal is © The Royal Society of Chemistry 2012

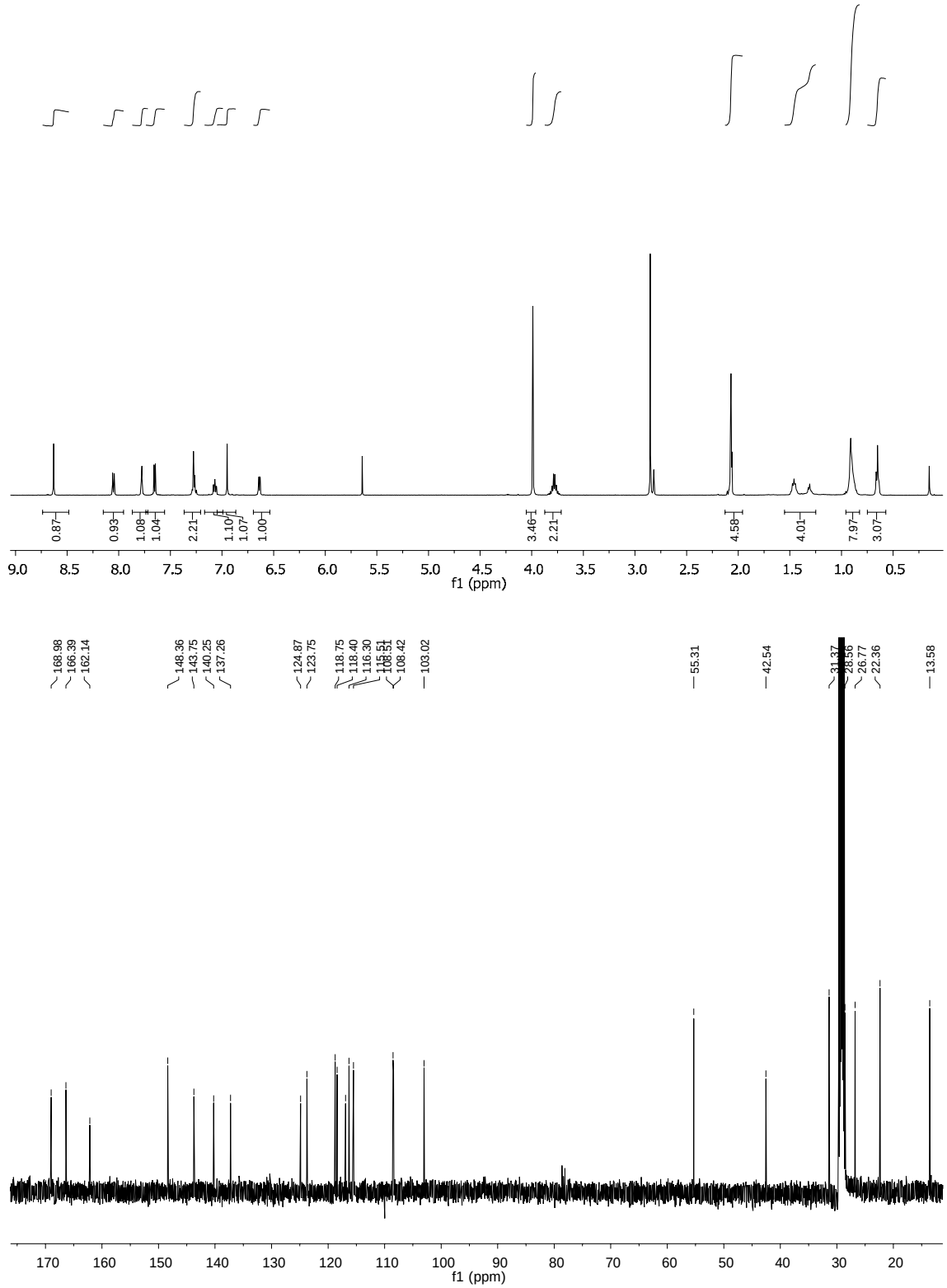

Figure S2. ^{1}H and ^{13}C NMR spectra of **1c** in $(CD_3)_2C(O)$.

This journal is © The Royal Society of Chemistry 2012

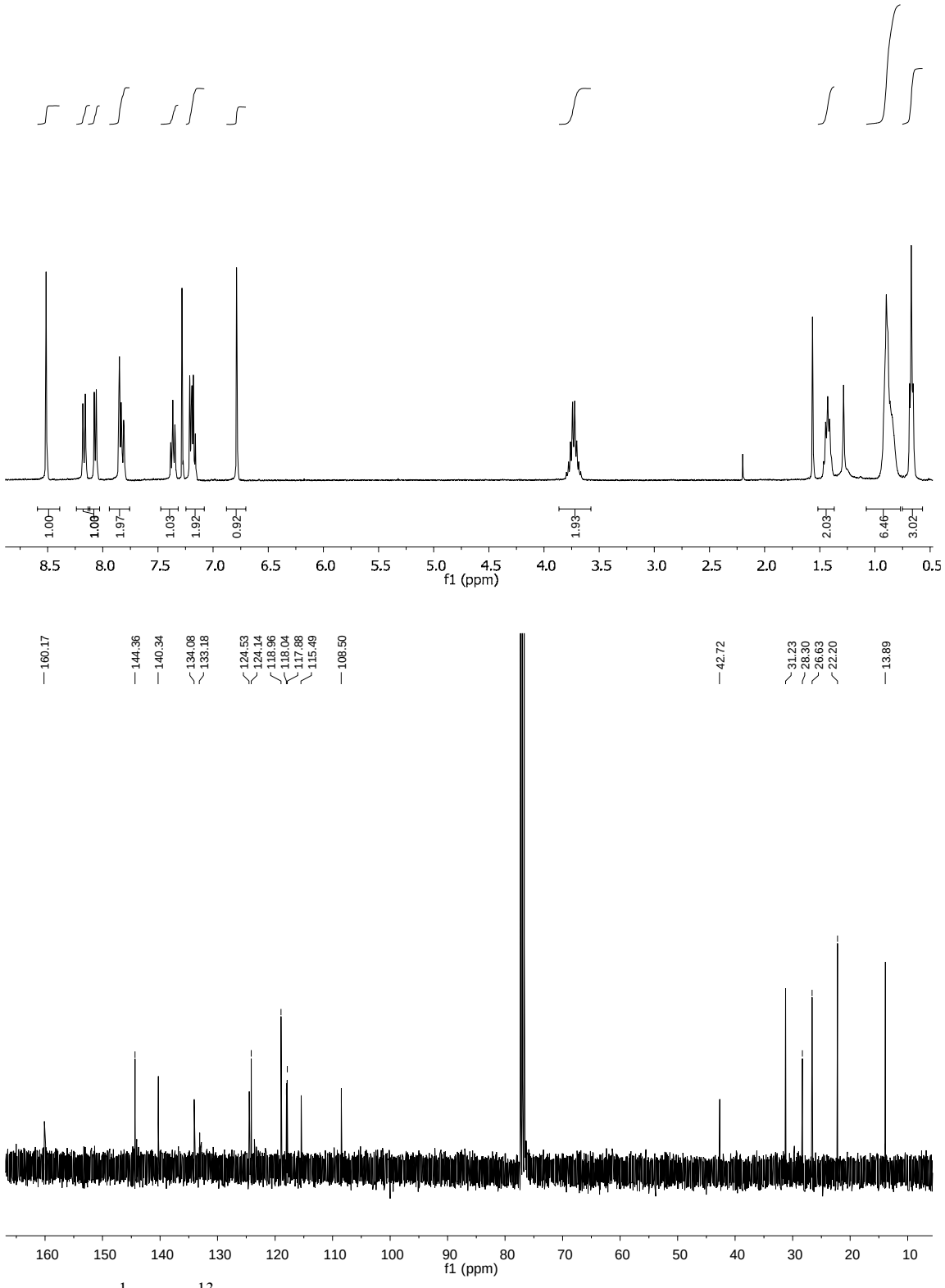

Figure S3. ^{1}H and ^{13}C NMR spectra of **1d** in $CDCl_3$.

This journal is © The Royal Society of Chemistry 2012

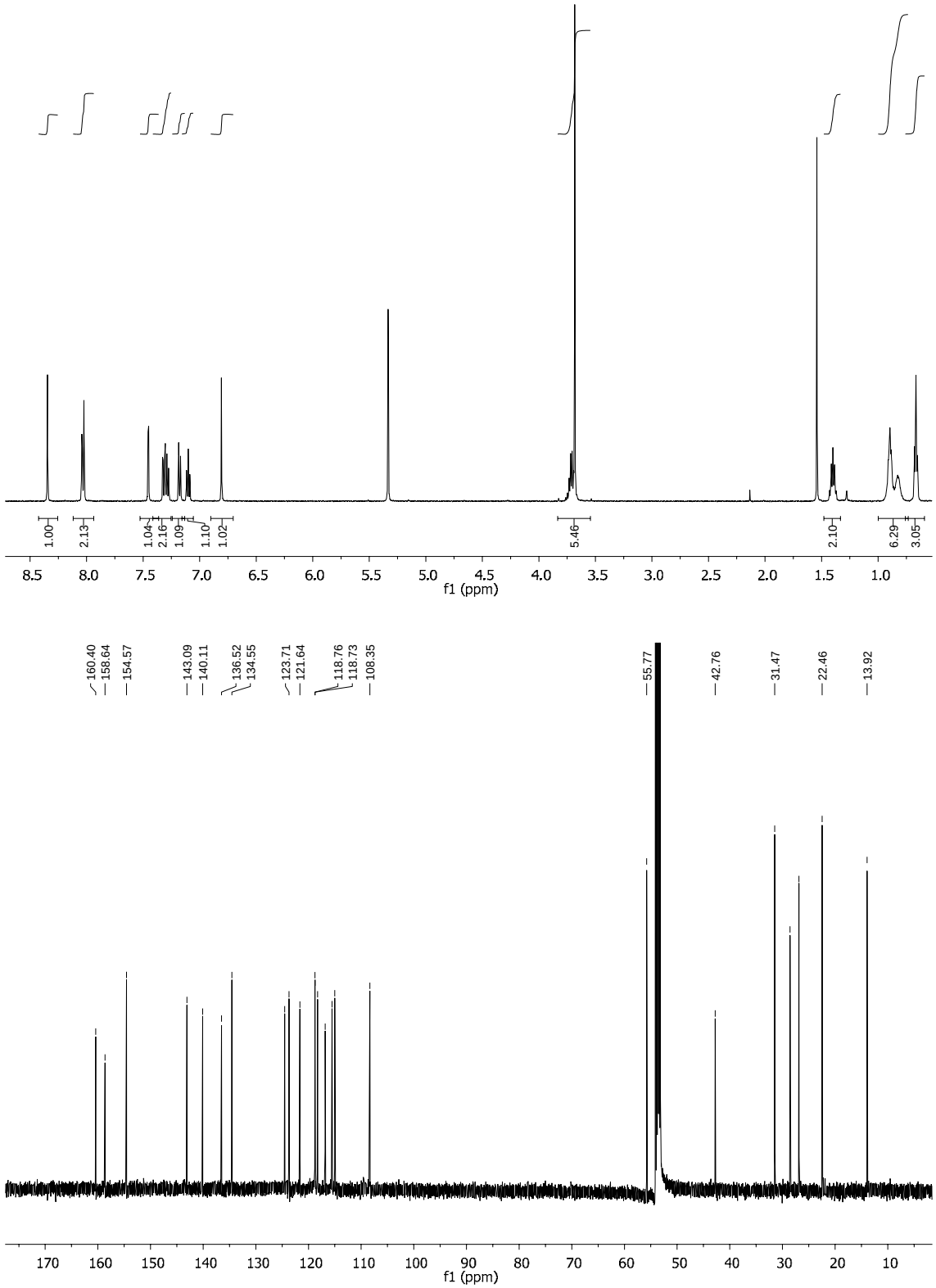

Figure S4. ^{1}H and ^{13}C NMR spectra of **1e** in CD_2Cl_2.

This journal is © The Royal Society of Chemistry 2012

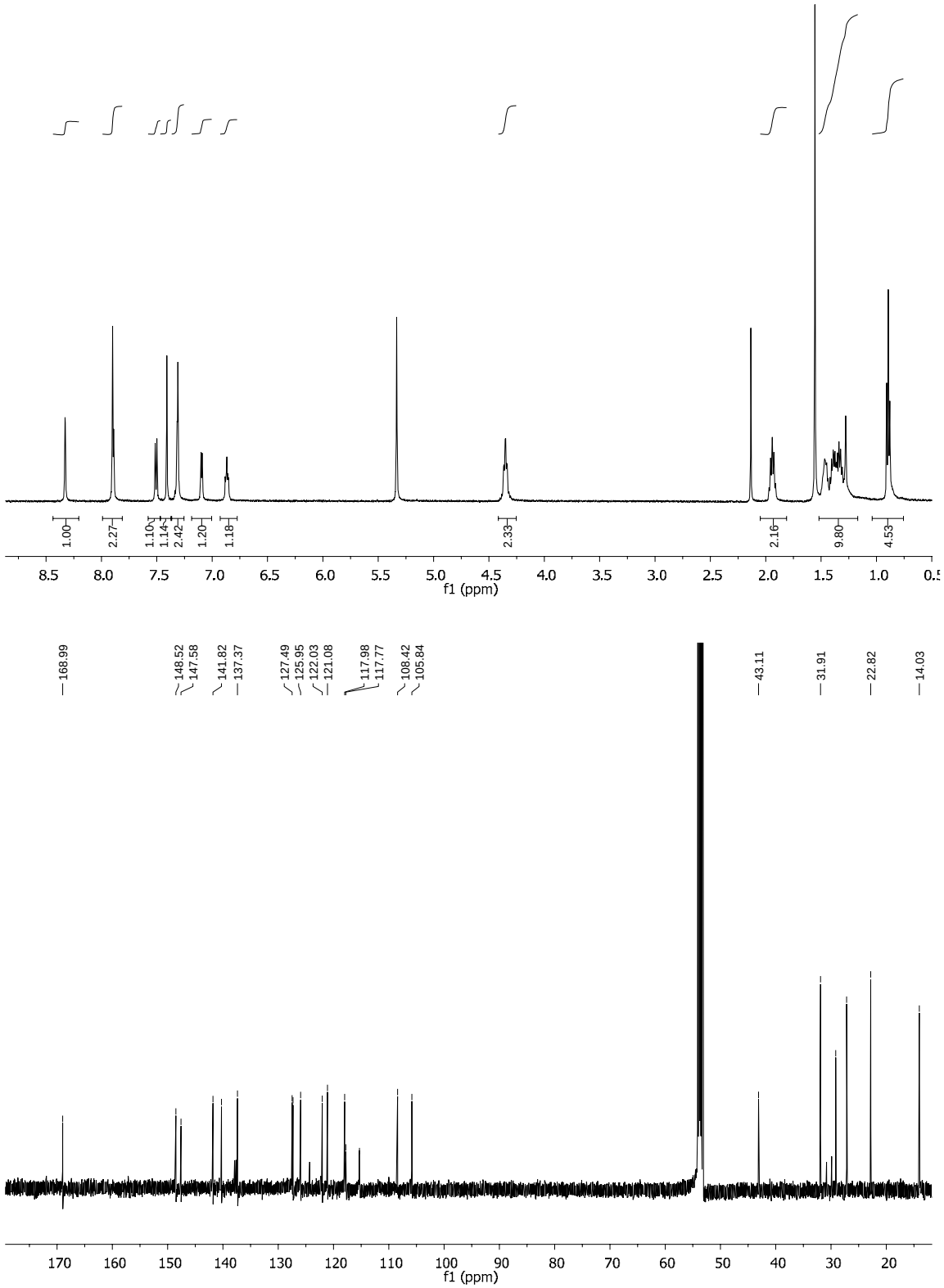

Figure S5. ^{1}H and ^{13}C NMR spectra of **2b** in CD_2Cl_2.

This journal is © The Royal Society of Chemistry 2012

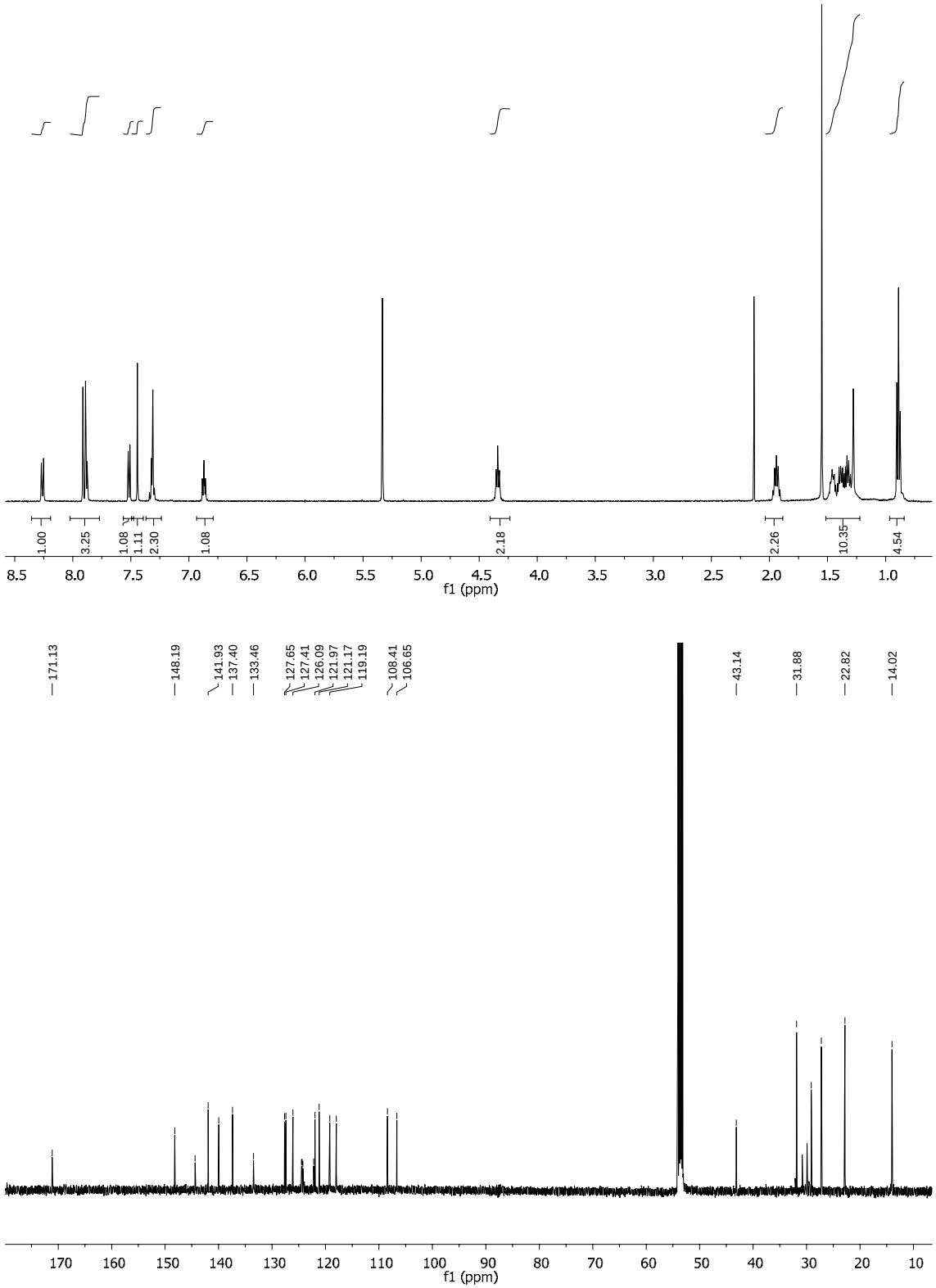

Figure S6. ^{1}H and ^{13}C NMR spectra of **2d** in CD_2Cl_2.

This journal is © The Royal Society of Chemistry 2012

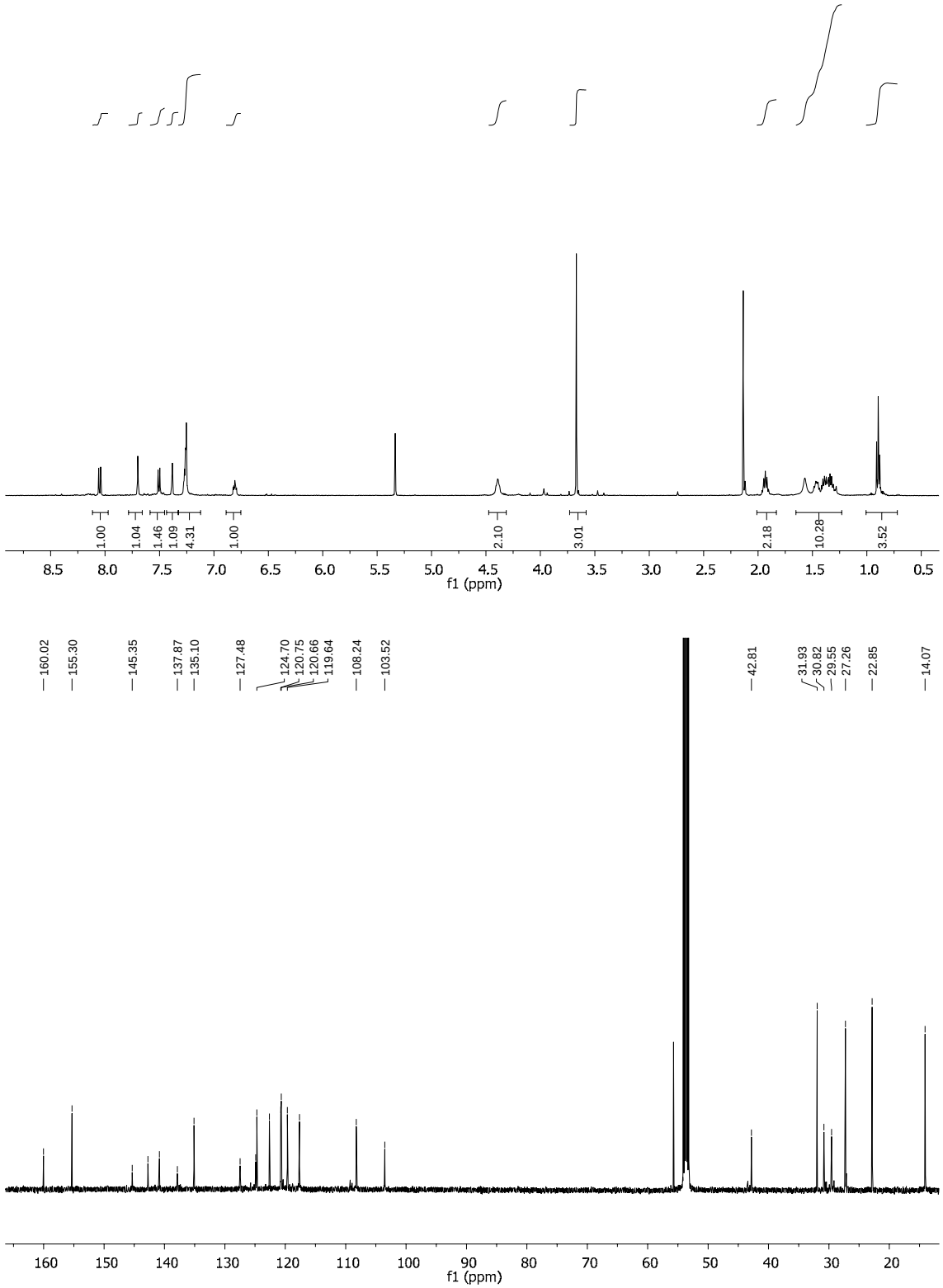

Figure S7. ^{1}H and ^{13}C NMR spectra of **2e** in CD_2Cl_2.

This journal is © The Royal Society of Chemistry 2012

Computational Studies

General

All computations were carried out with the Gaussian 03 and 09 packages.[3,4] The choice of functional for $Ir(ppy)_3$ and related derivatives has been the popular B3LYP[5] hybrid functional, presumably selected on the basis of Hay's theoretical study on $Ir(ppy)_3$ reported in 2002.[6] The basis sets used in the Hay study were the LANL2DZ pseudopotential for the iridium atom and 6-31G for other atoms. These model chemistries have been used in many subsequent investigations of related iridium complexes.[7] There is recent debate as to whether the B3LYP functional is appropriate for such complexes since many other DFT functionals exist.[8,9]

Table S1 shows a comparison of computed data from selected functionals and basis sets with experimental data for $Ir(ppy)_3$. The geometrical data from B3LYP and various basis sets with gas-phase electron diffraction data for $Ir(ppy)_3$ are in good agreement with the pseudopotential LANL2DZ[10] for Ir and the 3-21G* basis set[11] for other atoms being the best fit of the four basis sets studied. Changing the B3LYP functional at the LANL2DZ : 3-21G* basis set to PBE0,[12] MPW1K[13] and CAM-B3LYP[14] reveal optimised geometries that do not fit as well with the experimental gas-phase geometry.

Comparing the calculated MO and photophysical energies from the various DFT hybrid functionals with observed CV and photophysical data for $Ir(ppy)_3$ in Table S1, experimental and computed energies are different for many reasons, e.g. external effects such as solvent and temperature which do not exist in the 'gas-phase' calculations. The different functionals and basis sets also markedly influence these energy values. The observation that the B3LYP functional gives better energy matches is perhaps the reason why the B3LYP functional remains the choice for many investigations into the photophysics of iridium complexes. It is well known that different scaling factors have been used to correct the vibration energies[15] and NMR shifts[16] computed by different functionals and basis sets in order to make realistic experiment vs theory comparisons. These factors may well be applicable to MO and TD-DFT energies (*vide infra*).

Electronic Supplementary Material (ESI) for Journal of Materials Chemistry
This journal is © The Royal Society of Chemistry 2012

Table S1. Comparison of computed data from selected model chemistries with reported experimental data for $Ir(ppy)_3$.

Pseudopotential for Ir Basis set for other atoms	Expt. data	B3LYP LANL2DZ LANL2DZ	B3LYP LANL2DZ 6-31G	B3LYP LANL2DZ 3-21G*	B3LYP LANL2DZ 6-31G*	PBE0 LANL2DZ 3-21G*	MPW1K LANL2DZ 3-21G*	CAM- B3LYP LANL2DZ 3-21G*
Ir-N bond length (Å)	2.033(6)[a]	2.035	2.036	2.032	2.027	2.011	2.008	2.025
Ir-C bond length (Å)	2.158(2)[a]	2.151	2.167	2.150	2.189	2.115	2.111	2.135
LUMO (eV)	-2.10[b]	-1.47	-1.23	-1.23	-1.20	-1.13	-0.55	0.03
HOMO (eV)	-5.11[b]	-4.95	-4.79	-4.84	-4.85	-5.12	-5.90	-6.17
HLG (eV)	3.01[b]	3.48	3.56	3.61	3.65	3.99	5.35	6.20
$S_0 > T_1$ (absorption, nm)	488[c]	494	480	471	470	461	460	431
$S_0 > S_1$ (absorption, nm)	455[c]	447	444	437	428	413	354	349

[a] From gas-phase electron-diffraction data for $Ir(ppy)_3$ at 658 K; reference [17].

[b] From CV data on $Ir(ppy)_3$ in DMF and values in volts(V) based on 4.8 V for the FcH/FcH^+ couple; reference [18].

[c] From absorption data for $Ir(ppy)_3$ in DCM – these are very weak mixed MLCT bands that are described as a mixture of $S_0 > T_n$ n=1-3, $S_0 > S_n$ n=1-3 transitions due to spin-orbit coupling – 'assigned' as ^{3}MLCT and ^{1}MLCT for 488 and 455 nm, respectively; reference 18.

Electronic Supplementary Material (ESI) for Journal of Materials Chemistry
This journal is © The Royal Society of Chemistry 2012

Optimised geometries

All optimised S_0 geometries of the series **1** and **2** iridium complexes, with the hexyl groups replaced by methyl groups to reduce computational time without fundamentally affecting the computed electronic structures and photophysical data, in this study have near C_3 symmetries (Table S2). All were found to be true minima based on no imaginary frequencies found. Compound **1a** has been structurally characterized by single crystal X-ray diffraction[19] and is in good agreement with the geometry **1a'** at the B3LYP / LANL2DZ : 3-21G* model chemistry.

Table S2. Comparison of selected bond parameters for optimised and experimental geometries of series **1'** and **2'**. The LANL2DZ pseudopotential is used for iridium.

Compound	Basis set for all atoms except Ir	Ir-C bond length (Å)	Ir-N bond length (Å)
1a'	LANL2DZ	2.036	2.149
1a'	3-21G*	2.032	2.147
1a'	6-31G	2.036	2.164
1a'	6-31G*	2.035	2.184
1a	*X-ray (averaged)*	*2.017(5)*	*2.128(5)*
1b'	3-21G*	2.033	2.144
1c'	3-21G*	2.031	2.150
1d'	3-21G*	2.032	2.143
1e'	3-21G*	2.033	2.147
2a'	3-21G*	2.037	2.145
2b'	3-21G*	2.038	2.141
2c'	3-21G*	2.036	2.148
2d'	3-21G*	2.036	2.142
2e'	3-21G*	2.038	2.144

The influence of the different carbazole groups and substituents on the Ir-C and Ir-N bond lengths is small. The T_1 optimised geometries at the B3LYP/LANL2DZ:3-21G* level of theory for all iridium complexes here were of C_1 symmetries with variations of 0.03 – 0.06 Å for the Ir-C and Ir-N bond lengths (Table S3). These distortions have been noted for the optimised triplet state geometries for $Ir(ppy)_3$ elsewhere.[6,20,21,22,23] The optimised singlet excited state (S_1) geometries for $Ir(ppy)_3$, **1a'** and **2a'** were also obtained and shown to have similar C_1 symmetries as the T_1 optimised geometries with similar energies (Table S4).

Electronic Supplementary Material (ESI) for Journal of Materials Chemistry
This journal is © The Royal Society of Chemistry 2012

Table S3. Selected bond lengths from S_0, T_1 and S_1 optimised geometries of $Ir(ppy)_3$, **1a'** and **2a'**.

	$Ir(ppy)_3$	**1a'**	**2a'**	$Ir(ppy)_3$	**1a'**	**2a'**
	Ir-C	Ir-C	Ir-C	Ir-N	Ir-N	Ir-N
S_0	2.031	2.031	2.036	2.149	2.143	2.144
	2.031	2.033	2.037	2.150	2.147	2.145
	2.032	2.033	2.038	2.150	2.152	2.145
T_1	1.993	2.015	1.986	2.111	2.098	2.137
	2.024	2.022	2.038	2.170	2.156	2.153
	2.047	2.046	2.047	2.175	2.160	2.164
S_1	1.991	1.975	1.970	2.148	2.142	2.151
	2.035	2.036	2.045	2.173	2.167	2.162
	2.038	2.047	2.048	2.175	2.172	2.165

Table S4. Relative energies (in eV) of optimised geometries for complexes discussed in this study.

	$Ir(ppy)_3$	**1a'**	**1b'**	**1c'**	**1d'**	**1e'**	**2a'**	**2b'**	**2c'**	**2d'**	**2e'**
T_1-S_0	2.56	2.58	2.32	2.72	2.37	2.50	2.20	1.99	2.24	2.03	2.28
S_0-$S_0(T_1)$	0.25	0.27	0.19	0.24	0.22	0.34	0.22	0.19	0.21	0.20	0.26
T_1-$T_1(S_0)$	0.25	0.31	0.27	0.24	0.26	0.33	0.53	0.26	0.26	0.36	0.24
Av	0.25	0.29	0.23	0.24	0.24	0.34	0.37	0.23	0.24	0.28	0.25
$T_1(S_0) - S_1(S_0)$	0.09	0.08					0.09				

MO computations

Electronic structure and frequency calculations were also carried out at the B3LYP/LANL2DZ:3-21G* level of theory. The MO diagrams and orbital contributions were generated with the aid of Gabedit[24] and GaussSum[25] packages, respectively.

The electronic structures computed, assuming S_0 ground states, for both S_0 and T_1 optimised geometries of $Ir(ppy)_3$ are similar except for two points. (Figure S8 and Table S5) The frontier orbitals are important for our understanding of the nature of the phosphorescence emission which is mainly $S_0 < T_1$. Firstly, as noted elsewhere,[16,18] the unoccupied π_1*, π_{2a}* and π_{2b}* orbitals are localised on one pyridyl group for the optimised T_1 geometry whereas for the optimised S_0 geometry the orbitals are delocalised over two or three pyridyl groups. This is inevitable as the T_1 geometry is less symmetrical than S_0. The contribution of metal and the phenyl ring character increases by 9% in the LUMO at the expense of the pyridyl ring character for the T_1 geometry compared to the LUMO for the S_0 geometry. Secondly, the LUMO π_1* is ca 0.2 eV lower in energy in the T_1 geometry than in the optimised S_0 geometry.

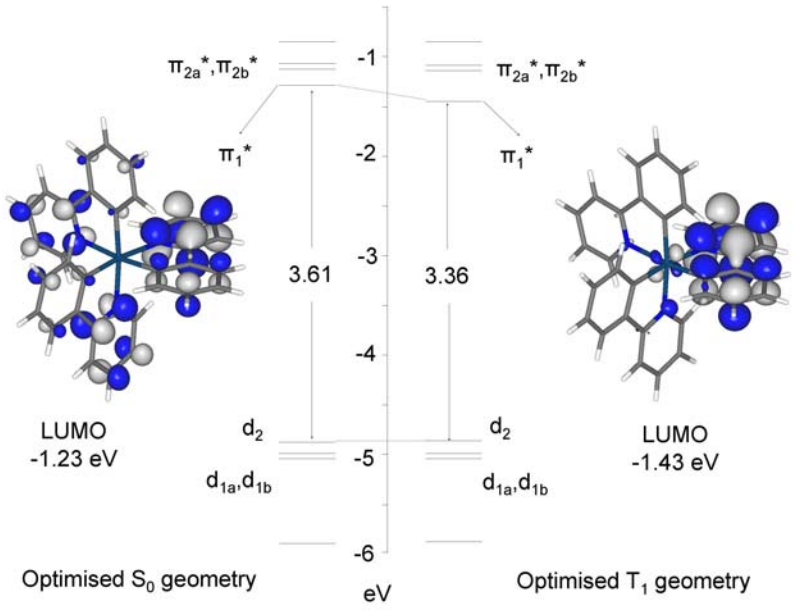

Figure S8. Orbital energies for S_0 and T_1 optimised geometries of $Ir(ppy)_3$ along with the delocalised and localised LUMOs for both geometries.

Electronic Supplementary Material (ESI) for Journal of Materials Chemistry
This journal is © The Royal Society of Chemistry 2012

Table S5. Orbital energies and detailed compositions for S_0 and T_1 optimised geometries of $Ir(ppy)_3$

At optimised S_0 geometry

MO		eV	Ir	py1	py2	py3	ph1	ph2	ph3	Ir	py	ph	Ir+ph	py
134	LUMO+3	-0.85	2	32	30	26	4	3	2	2	88	9	11	88
133	LUMO+2	-1.11	5	3	17	53	1	5	17	5	73	23	28	73
132	LUMO+1	-1.14	5	31	36	6	9	11	2	5	73	22	27	73
131	LUMO	-1.23	1	39	20	14	13	7	5	1	73	25	26	73
130	HOMO	-4.84	53	3	2	3	11	10	18	53	8	39	92	8
129	HOMO-1	-5.00	44	3	3	4	8	13	24	44	10	45	89	10
128	HOMO-2	-5.03	45	3	5	2	23	20	2	45	10	45	90	10
127	HOMO-3	-5.92	3	3	3	17	12	8	55	3	23	75	78	23

At optimised T_1 geometry

MO		eV	Ir	py1	py2	py3	ph1	ph2	ph3	Ir	py	ph	Ir+ph	py
134	LUMO+3	-0.82	2	8	39	40	1	5	5	2	87	11	13	87
133	LUMO+2	-1.17	5	1	20	53	0	6	15	5	74	21	26	74
132	LUMO+1	-1.19	4	4	50	18	2	16	6	4	72	24	28	72
131	LUMO	-1.43	4	59	3	3	29	1	1	4	65	31	35	65
130	HOMO	-4.79	48	8	2	2	23	5	13	48	12	41	89	12
129	HOMO-1	-5.06	41	7	2	3	21	4	21	41	12	46	87	12
128	HOMO-2	-5.09	45	1	4	4	3	35	8	45	9	46	91	9
127	HOMO-3	-5.87	8	23	2	2	52	7	7	8	27	66	74	27

These S_0 vs T_1 MO trends also apply to the electronic structures calculated for the **1'** series as shown in Tables S6, S6 and Figure S9. However, for the **2'** series the HOMO energies are higher by ca 0.2 eV in the T_1 geometries compared to the S_0 geometries. The energies for the LUMOs are ca 0.1 eV lower in the T_1 geometries compared to the S_0 geometries for the **2'** series.

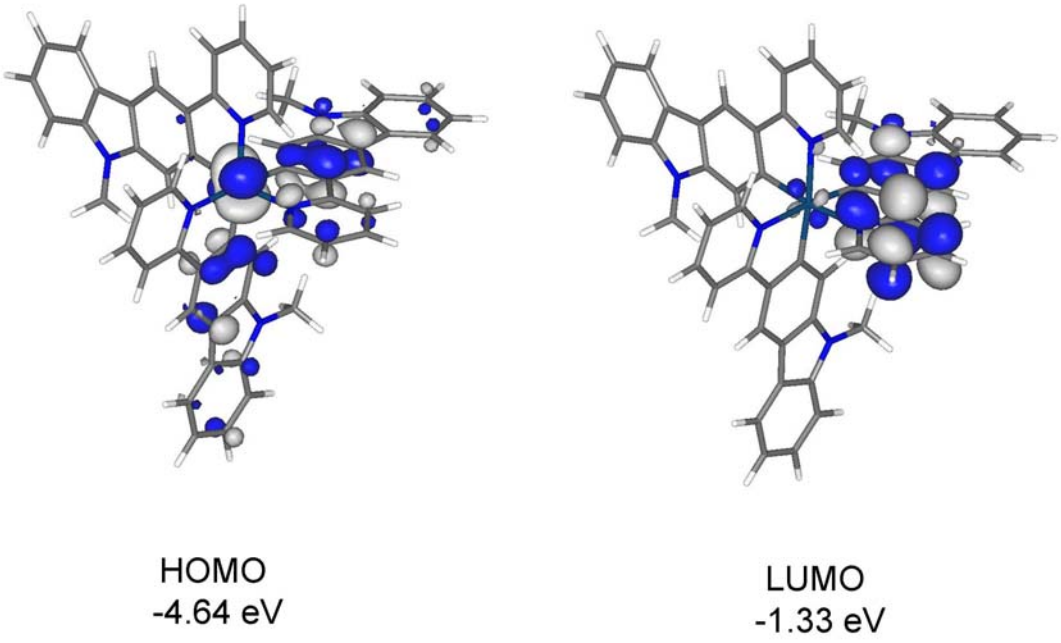

1a'

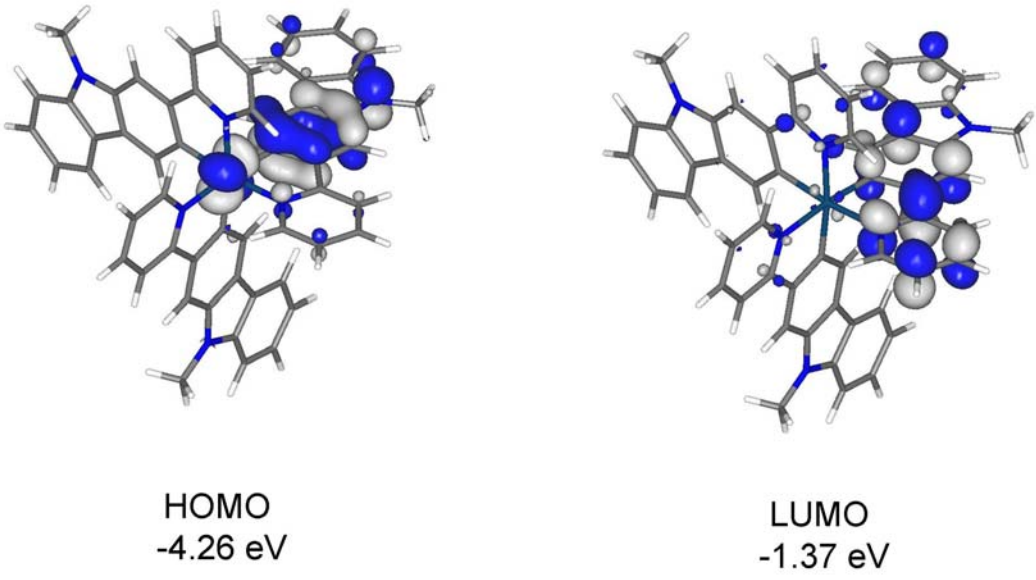

2a'

Figure S9. Frontier orbitals (HOMO and LUMO) for the T_1 optimised geometries for **1a'** and **2a'** showing the *localised* orbitals.

This journal is © The Royal Society of Chemistry 2012

Table S6. MO energies and MO compositions of Ir, pyridyl and carbazolyl character in % for complexes **1a'-e'**, **2a'-e'**and $Ir(ppy)_3$.

		$Ir(ppy)_3$				**1a'**				**2a'**			
MO		eV	Ir	py	ph	eV	Ir	py	cz	eV	Ir	py	cz
LUMO+3	π_3*	-0.85	2	88	9	-0.82	2	80	17	-0.82	2	89	8
LUMO+2	π_{2b}*	-1.11	5	73	23	-1.03	4	73	23	-1.16	4	61	35
LUMO+1	π_{2a}*	-1.14	5	73	22	-1.05	4	73	22	-1.17	4	60	35
LUMO	π_1*	-1.23	1	73	25	-1.12	1	72	26	-1.27	1	59	41
HOMO	d_2	-4.84	53	8	39	-4.70	39	8	53	-4.44	31	5	64
HOMO-1	d_{1a}	-5.00	44	10	45	-4.80	28	6	68	-4.48	22	4	72
HOMO-2	d_{1b}	-5.03	45	10	45	-4.82	29	5	67	-4.49	22	5	72
HOMO-3	π	-5.92	3	23	75	-5.00	3	11	86	-5.15	6	10	85

		1b'				**1c'**				**1d'**				**1e'**			
MO		eV	Ir	py	cz	eV	Ir	py	cz	eV	Ir	py	cz	eV	Ir	py	cz
LUMO+3	π_3*	-1.39	1	72	27	-0.57	2	90	6	-1.35	2	91	9	-0.72	2	64	35
LUMO+2	π_{2b}*	-1.77	5	83	11	-0.72	2	63	34	-1.65	3	72	25	-1.01	5	81	15
LUMO+1	π_{2a}*	-1.78	5	83	12	-0.72	2	63	33	-1.70	4	72	24	-1.03	5	81	15
LUMO	π_1*	-1.85	2	86	12	-0.84	1	61	39	-1.78	1	72	27	-1.08	2	85	12
HOMO	d_2	-5.11	36	8	56	-4.53	42	9	49	-5.14	36	8	57	-4.63	34	12	54
HOMO-1	d_{1a}	-5.18	22	4	74	-4.63	33	6	62	-5.21	23	4	73	-4.76	24	8	69
HOMO-2	d_{1b}	-5.19	23	5	73	-4.63	33	6	60	-5.22	23	4	73	-4.77	24	7	68
HOMO-3	π	-5.35	5	11	83	-4.85	1	11	88	-5.39	4	14	83	-4.91	5	13	82

This journal is © The Royal Society of Chemistry 2012

		2b'				**2c'**				**2d'**				**2e'**			
MO		eV	Ir	py	cz	eV	Ir	py	cz	eV	Ir	py	cz	eV	Ir	py	cz
LUMO+3	π_3*	-1.26	2	92	6	-0.50	3	95	3	-1.50	2	72	25	-0.69	2	81	16
LUMO+2	π_{2b}*	-1.72	4	64	33	-0.86	2	52	47	-1.81	5	77	17	-0.84	4	63	32
LUMO+1	π_{2a}*	-1.76	4	63	33	-0.89	3	51	46	-1.85	6	76	17	-0.87	4	61	35
LUMO	π_1*	-1.87	1	64	35	-1.02	1	51	48	-1.92	2	79	19	-0.94	1	58	41
HOMO	d_2	-4.82	28	4	68	-4.22	35	5	60	-4.82	21	5	74	-4.21	32	7	62
HOMO-1	d_{1a}	-4.86	20	4	76	-4.27	27	4	68	-4.86	19	4	77	-4.28	25	5	70
HOMO-2	d_{1b}	-4.86	20	4	75	-4.29	27	6	67	-4.89	19	4	77	-4.32	26	6	67
HOMO-3	π	-5.51	7	10	83	-4.99	5	10	84	-5.49	6	10	83	-4.88	1	17	81

Electronic Supplementary Material (ESI) for Journal of Materials Chemistry
This journal is © The Royal Society of Chemistry 2012

Table S7. Molecular orbital energies and compositions for the series **1'** and **2'** at optimised T_1 geometries.

	1a'				**1b'**				**1c'**				**1d'**				**1e'**			
MO	eV	Ir	py	cz	eV	Ir	py	cz	eV	Ir	py	cz	eV	Ir	py	cz	eV	Ir	py	cz
LUMO+3	-0.78	2	80	18	-1.37	2	73	26	-0.51	2	89	8	-1.32	2	89	8	-0.71	2	64	34
LUMO+2	-1.05	4	73	23	-1.79	4	83	12	-0.70	2	64	34	-1.67	3	72	26	-1.03	5	80	15
LUMO+1	-1.09	3	73	25	-1.82	4	84	12	-0.77	2	62	37	-1.74	3	72	26	-1.05	3	83	14
LUMO	-1.33	3	64	33	-2.11	5	79	17	-1.06	2	57	41	-1.94	2	67	31	-1.34	4	73	24
HOMO	-4.64	35	11	53	-5.06	32	9	59	-4.45	41	11	49	-5.09	34	10	56	-4.56	30	16	53
HOMO-1	-4.85	29	6	66	-5.24	22	6	72	-4.63	35	7	58	-5.22	24	4	72	-4.80	21	10	69
HOMO-2	-4.86	28	6	66	-5.25	21	5	74	-4.64	33	8	59	-5.25	22	5	73	-4.82	22	9	68
HOMO-3	-5.01	4	14	83	-5.39	4	13	83	-4.85	1	11	88	-5.40	6	11	84	-4.92	7	13	79

	2a'				**2b'**				**2c'**				**2d'**				**2e'**			
MO	eV	Ir	py	cz	eV	Ir	py	cz	eV	Ir	py	cz	eV	Ir	py	cz	eV	Ir	py	cz
LUMO+3	-0.77	2	90	9	-1.47	2	73	25	-0.47	3	95	3	-1.36	2	94	5	-0.71	2	80	18
LUMO+2	-1.15	4	60	36	-1.83	5	77	18	-0.87	2	51	46	-1.83	3	64	32	-0.89	4	65	31
LUMO+1	-1.19	3	58	39	-1.86	5	77	20	-0.94	2	50	47	-1.86	4	63	33	-0.93	4	64	32
LUMO	-1.37	2	54	44	-2.04	3	71	26	-1.14	2	48	50	-2.00	1	62	37	-1.10	2	54	43
HOMO	-4.26	28	7	64	-4.69	23	6	71	-4.07	30	8	62	-4.66	20	6	73	-4.09	25	9	65
HOMO-1	-4.44	27	6	68	-4.85	20	4	75	-4.25	29	6	65	-4.88	21	4	75	-4.29	25	6	69
HOMO-2	-4.47	25	5	71	-4.89	20	4	76	-4.29	29	4	66	-4.94	20	3	76	-4.33	24	5	70
HOMO-3	-5.16	5	10	84	-5.52	6	11	85	-5.01	5	10	85	-5.56	5	11	83	-4.89	1	21	78

The trends in the HOMO energies at S_0 geometries are reflected in the CV data for these complexes as shown in Table 1 (in the manuscript) and Figure S10 where there are very good correlations within each series.

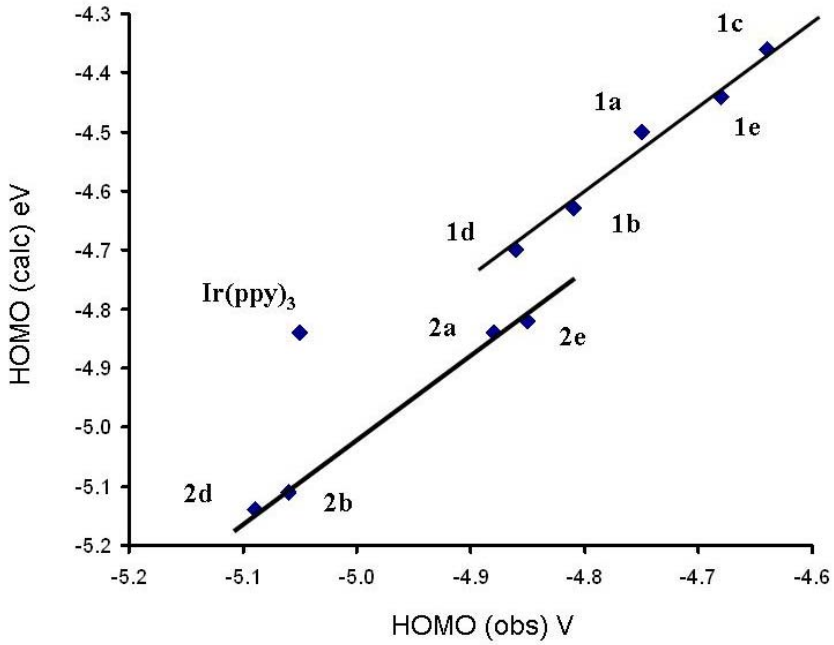

Figure S10. Correlation between observed and computed HOMO energies.

TD-DFT computations

The time-dependent DFT (TD-DFT) method assumes that the geometry at S_0 would be the same as the geometries found in the excited states.[14] If the S_0 optimised geometry is considerably different to the T_1 optimised geometry then TD-DFT will overestimate the energies for $S_0 > T_1$ transitions if the S_0 optimised geometry is used. Conversely TD-DFT will underestimate the energies for $S_0 > T_1$ transitions if the T_1 optimised geometry is used. The degree of over- and under-estimation depends on how different the two geometries are. The differences may be estimated by calculating the energy differences for both geometries as S_0 geometries or both geometries as T_1 geometries.

The TD-DFT method does not include spin-orbit couplings thus does not give oscillation strengths for the triplet excited states and does not compute mixed singlet-triplet excited states.[14] It does not include solvent and temperature effects. It is believed that mixed excited states would result in lower energy transitions[15] (a

difference of -0.08 eV is found by comparing with the lowest energy transition S_0 > T_1 for $Ir(ppy)_3$ at the same level of theory i.e. B3PW91/LANL2DZ) whereas solvent effects would result in higher energy transitions (a difference of +0.07 eV is found here for $Ir(ppy)_3$ in dichloromethane solution compared to in the gas phase at the B3LYP/LANL2DZ:3-21G* level of theory). Both modifications would effectively cancel each other thus the gas-phase TD-DFT data given here are conveniently appropriate. As explained earlier, one disadvantage with the general TD-DFT method is it assumes all excited state geometries to have the same geometries. The energy differences in the S_0 and T_1 optimised geometries for the iridium complexes here are in the region of 0.2-0.4 eV (Table S4) which are larger than the energy differences observed from solvent and spin-orbit coupling effects.

Detailed TD-DFT data on the optimised S_0 and T_1 geometries of $Ir(ppy)_3$ are listed in Table S8. The nature of the lowest energy transitions of interest is reproduced for all iridium complexes as listed in Tables S9 and S10. Transitions for $Ir(ppy)_3$ are discussed here as examples. In the S_0 geometry the three triplet state transitions of lowest energy (S_0>T_1, S_0>T_2, S_0>T_3) are close together within 0.05 eV while the lowest energy singlet state transition (S_0>S_1) is 0.27 eV higher in energy compared to the triplet state transitions. In the T_1 geometry for $Ir(ppy)_3$ the S_0>T_1 transition is 0.47 eV lower than the S_0>T_2 transition and 0.35 eV lower than the S_0>S_1 transition. This shows that each geometry somewhat influences the transition energies. However, the nature of the many transitions of low energies in $Ir(ppy)_3$ is shown to be similar for all states with 40-52% metal and 9-21% phenyl character at the ground states and 52-65% pyridyl character at the excited states. For series **1** and **2** the many transitions of low energies for all states are also similar in nature with 21-32% metal and 60-74% carbazolyl character at the ground states and 50-84% pyridyl character at the excited states.

Electronic Supplementary Material (ESI) for Journal of Materials Chemistry
This journal is © The Royal Society of Chemistry 2012

Table S8. Nature of lowest energy transitions (S_0>S_n and S_0>T_n) from TD-DFT computations from optimised S_0 and T_1 geometries of $Ir(ppy)_3$.

From S_0 geometry

State	eV	nm	*f*	Major contributions	Ir	py	ph
T_1	2.63	471	0.000	HOMO->LUMO (73%)	48-->2 (-46)	10-->73 (63)	42-->25 (-17)
T_2	2.66	467	0.000	HOMO->LUMO+2 (58%)	48-->5 (-43)	10-->73 (63)	43-->23 (-20)
T_3	2.68	464	0.000	HOMO->LUMO+1 (48%)	48-->4 (-44)	10-->73 (63)	42-->23 (-19)
S_1	2.84	437	0.005	HOMO->LUMO (93%)	53-->1 (-52)	8-->73 (65)	39-->26 (-13)
S_2	2.89	429	0.002	HOMO->LUMO+1 (93%)	53-->5 (-48)	8-->73 (65)	39-->22 (-17)
S_3	2.92	424	0.003	HOMO->LUMO+2 (94%)	53-->5 (-48)	8-->73 (65)	39-->22 (-17)
S_4	3.07	404	0.021	HOMO-1->LUMO (77%)	44-->2 (-42)	10-->73 (63)	46-->26 (-20)
S_5	3.09	402	0.007	HOMO-2->LUMO (-37%), HOMO-1->LUMO+1 (41%)	45-->4 (-41)	10-->73 (63)	45-->24 (-21)
S_6	3.13	397	0.030	HOMO-2->LUMO (38%)	45-->3 (-42)	10-->73 (63)	45-->24 (-21)

From T_1 geometry

State	eV	nm	*f*	Major contributions	Ir	py	ph
T_1	2.16	573	0.000	HOMO->LUMO (89%)	44-->4 (-40)	13-->65 (52)	43-->31 (-12)
S_1	2.51	493	0.009	HOMO->LUMO (93%)	48-->4 (-44)	12-->65 (53)	40-->31 (-9)
T_2	2.63	471	0.000	HOMO->LUMO+1 (-25%), HOMO->LUMO+2 (38%)	45-->4 (-41)	12-->72 (60)	43-->24 (-19)
T_3	2.65	468	0.000	HOMO->LUMO+1 (46%), HOMO->LUMO+2 (22%)	45-->4 (-41)	12-->72 (60)	43-->24 (-19)
S_2	2.80	444	0.003	HOMO->LUMO+1 (90%)	48-->4 (-44)	12-->73 (61)	40-->23 (-17)
S_3	2.83	437	0.004	HOMO->LUMO+2 (83%)	48-->5 (-43)	12-->73 (61)	41-->23 (-18)
S_4	2.86	434	0.005	HOMO-2->LUMO (86%)	45-->4 (-41)	10-->66 (56)	45-->30 (-15)
S_5	2.98	416	0.077	HOMO-1->LUMO (85%)	41-->3 (-38)	12-->66 (54)	47-->30 (-17)
S_6	3.06	405	0.006	HOMO-2->LUMO+1 (48%), HOMO-1->LUMO+1 (25%)	43-->4 (-39)	11-->73 (62)	46-->23 (-23)

Electronic Supplementary Material (ESI) for Journal of Materials Chemistry
This journal is © The Royal Society of Chemistry 2012

Table S9. Nature of the lowest energy transitions ($S_0 > T_1$) from TD-DFT computations from optimised S_0 geometries of iridium complexes. The values in parentheses reflect the change in character of the iridium, pyridyl and carbazolyl groups on going from S_0 to T_1 states. In the case of $Ir(ppy)_3$ phenylene character values are given instead of carbazolyl character.

	eV	nm	Major contributions	Ir	pyridyl	carbazolyl
1a'	2.64	470	HOMO->LUMO (57%)	31-->2 (-29)	8-->72 (64)	61-->25 (-36)
1b'	2.41	514	HOMO->LUMO (40%), HOMO->LUMO+1 (24%)	29-->3 (-26)	8-->84 (76)	63-->12 (-51)
1c '	2.77	447	HOMO->LUMO (57%)	31-->1 (-30)	9-->63 (54)	62-->37 (-25)
1d '	2.49	499	HOMO->LUMO (63%)	28-->2 (-26)	8-->72 (64)	64-->26 (-38)
1e'	2.59	478	HOMO->LUMO (45%)	29-->3 (-26)	11-->83 (72)	60-->14 (-46)
2a'	2.27	547	HOMO->LUMO (66%)	28-->2 (-26)	5-->59 (54)	67-->39 (-28)
2b'	2.12	584	HOMO->LUMO (58%)	21-->3 (-18)	4-->78 (74)	76-->19 (-57)
2c '	2.32	533	HOMO->LUMO (66%)	32-->1 (-31)	6-->50 (44)	62-->48 (-14)
2d'	2.09	594	HOMO->LUMO (63%)	24-->2 (-22)	4-->64 (64)	74-->33 (-41)
2e'	2.37	524	HOMO->LUMO (62%)	29-->2 (-27)	7-->60 (53)	65-->38 (-27)
$Ir(ppy)_3$	2.63	471	HOMO->LUMO (73%)	48-->2 (-46)	10-->73 (63)	42-->25 (-17)

Electronic Supplementary Material (ESI) for Journal of Materials Chemistry
This journal is © The Royal Society of Chemistry 2012

Table S10. Nature of lowest energy transitions ($S_0 > T_1$) from TD-DFT computations on optimised T_1 geometries of iridium complexes

	eV	nm	Major contributions	Ir	pyridyl	carbazolyl
1a'	2.21	561	HOMO->LUMO (76%)	27-->3 (-24)	11-->64 (53)	62-->33 (-29)
1b'	2.00	621	HOMO->LUMO (82%)	27-->5 (-22)	9-->78 (69)	64-->17 (-47)
1c'	2.34	530	HOMO->LUMO (68%)	30-->2 (-28)	11-->57 (46)	60-->41 (-19)
1d'	2.16	574	HOMO->LUMO (76%)	26-->2 (-24)	10-->67 (57)	63-->31 (-32)
1e'	2.06	602	HOMO->LUMO (85%)	26-->4 (-22)	16-->73 (57)	58-->23 (-35)
2a'	1.87	662	HOMO->LUMO (97%)	28-->2 (-26)	7-->54 (47)	65-->44 (-21)
2b'	1.70	729	HOMO->LUMO (99%)	22-->3 (-19)	7-->71 (64)	71-->25 (-46)
2c'	1.92	645	HOMO->LUMO (98%)	30-->2 (-28)	8-->48 (40)	62-->51 (-11)
2d'	1.71	726	HOMO->LUMO (97%)	20-->1 (-19)	6-->62 (56)	73-->37 (-36)
2e'	1.93	644	HOMO->LUMO (98%)	24-->2 (-22)	10-->55 (45)	66-->43 (-23)
$Ir(ppy)_3$	2.16	573	HOMO->LUMO (89%)	44-->4 (-40)	13-->65 (52)	43-->31 (-12)

Electronic Supplementary Material (ESI) for Journal of Materials Chemistry
This journal is © The Royal Society of Chemistry 2012

Scaling Factors

A scaling factor may be used for one model chemistry to give more realistic energy values as in the case of observed and computed vibrational energies[15] and NMR shifts[16] elsewhere. This factor would be used to compute emission maxima in a specific solvent or solid state and at a specific temperature. A scaling factor of 0.925 is applied to the calculated emission maxima of the iridium complexes ($Ir(ppy)_3$, **1** and **2**) in this study (Table 3).

Table S11 lists the observed and predicted emission values for $Ir(ppy)_3$ and derivatives containing CF_3 and OMe groups with Figure S11 showing the numbering used. The observed emission energies were measured in ethanol/methanol glass at 77 K. The scaling factor used for this set is 0.954 and agreement is very good where possible. It is instructive to show the effect of an EWG or EDG substituent at different positions on the emission color and these trends are reflected in the emission maxima of series **1** and **2** complexes.

Scaling factors may also be used to accurately predict emission maxima using other model chemistries. Use of these factors is limited to compounds that have very similar geometries in both excited and ground states and thus have small Stokes shifts.

Table S11 Comparision between computed and observed emission energies for $Ir(ppy)_3$ and derivatives with CF_3 and OMe groups. (For numbering scheme see Figure S11).

$Ir(ppy)_3$ derivative	TD-DFT[a] (adjusted)	PL[b] (nm)
3-CF_3	472	
6-OMe	472	
7-OMe	486	
2-OMe	487	481
Parent	494	494
2-CF_3	494	494
7-CF_3	521	
6-CF_3	529	
3-OMe	541	539

[a]Scaling factor of 0.954 used on computed $S_0 > T_1$ energies.

[b]In ethanol/methanol glass at 77 K, reference [26].

Figure S11. Numbering scheme for $Ir(ppy)_3$

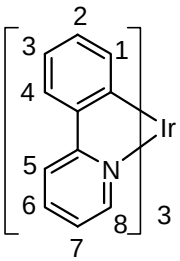

Electronic Supplementary Material (ESI) for Journal of Materials Chemistry
This journal is © The Royal Society of Chemistry 2012

References for the Supporting Information

1 S. D. Kuduk, R. M. DiPardo and M. G. Bock, *Org. Lett.*, 2005, **7**, 577.

2 S. Bettington, M. Tavasli, M. R. Bryce, A. Beeby, H. A. Al-Attar and A. P. Monkman, *Chem. Eur. J.* 2007, **13**, 1423.

3 Gaussian 03, Revision C.02, M. J. Frisch, G. W. Trucks, H. B. Schlegel, G. E. Scuseria, M. A. Robb, J. R. Cheeseman, J. A. Montgomery, Jr., T. Vreven, K. N. Kudin, J. C. Burant, J. M. Millam, S. S. Iyengar, J. Tomasi, V. Barone, B. Mennucci, M. Cossi, G. Scalmani, N. Rega, G. A. Petersson, H. Nakatsuji, M. Hada, M. Ehara, K. Toyota, R. Fukuda, J. Hasegawa, M. Ishida, T. Nakajima, Y. Honda, O. Kitao, H. Nakai, M. Klene, X. Li, J. E. Knox, H. P. Hratchian, J. B. Cross, C. Adamo, J. Jaramillo, R. Gomperts, R. E. Stratmann, O. Yazyev, A. J. Austin, R. Cammi, C. Pomelli, J. W. Ochterski, P. Y. Ayala, K. Morokuma, G. A. Voth, P. Salvador, J. J. Dannenberg, V. G. Zakrzewski, S. Dapprich, A. D. Daniels, M. C. Strain, O. Farkas, D. K. Malick, A. D. Rabuck, K. Raghavachari, J. B. Foresman, J. V. Ortiz, Q. Cui, A. G. Baboul, S. Clifford, J. Cioslowski, B. B. Stefanov, G. Liu, A. Liashenko, P. Piskorz, I. Komaromi, R. L. Martin, D. J. Fox, T. Keith, M. A. Al-Laham, C. Y. Peng, A. Nanayakkara, M. Challacombe, P. M. W. Gill, B. Johnson, W. Chen, M. W. Wong, C. Gonzalez and J. A. Pople, *Gaussian, Inc.*, Wallingford CT, 2004.

4 Gaussian 09, Revision A.02, M. J. Frisch, G. W. Trucks, H. B. Schlegel, G. E. Scuseria, M. A. Robb, J. R. Cheeseman, G. Scalmani, V. Barone, B. Mennucci, G. A. Petersson, H. Nakatsuji, M. Caricato, X. Li, H. P. Hratchian, A. F. Izmaylov, J. Bloino, G. Zheng, J. L. Sonnenberg, M. Hada, M. Ehara, K. Toyota, R. Fukuda, J. Hasegawa, M. Ishida, T. Nakajima, Y. Honda, O. Kitao, H. Nakai, T. Vreven, J. A. Montgomery, Jr., J. E. Peralta, F. Ogliaro, M. Bearpark, J. J. Heyd, E. Brothers, K. N. Kudin, V. N. Staroverov, R. Kobayashi, J. Normand, K. Raghavachari, A. Rendell, J. C. Burant, S. S. Iyengar, J. Tomasi, M. Cossi, N. Rega, J. M. Millam, M. Klene, J. E. Knox, J. B. Cross, V. Bakken, C. Adamo, J. Jaramillo, R. Gomperts, R. E. Stratmann, O. Yazyev, A. J. Austin, R. Cammi, C. Pomelli, J. W. Ochterski, R. L. Martin, K. Morokuma, V. G. Zakrzewski, G. A. Voth, P. Salvador, J. J. Dannenberg, S. Dapprich, A. D. Daniels, O. Farkas, J. B. Foresman, J. V. Ortiz, J. Cioslowski and D. J. Fox, *Gaussian, Inc.*, Wallingford CT, 2009.

5 (a) A. D. Becke, *J. Chem. Phys.,* 1993, **98**, 5648. (b) C. Lee, W. Yang and R. G. Parr, *Phys. Rev. B,* 1988, **37**, 785.

6 P. J. Hay, *J. Phys. Chem. A,* 2002, **106**, 1634.

Electronic Supplementary Material (ESI) for Journal of Materials Chemistry
This journal is © The Royal Society of Chemistry 2012

7 For examples of DFT computations on $Ir(ppy)_3$ and related complexes with the B3LYP functional, see (a) C.-F. Chang, Y.-M. Cheng, Y. Chi, Y.-C. Chiu, C.-C. Lin, G.-H. Lee, P.-T. Chou, C.-C. Chen, C.-H. Chang and C.-C. Wu, *Angew. Chem. Int. Ed.,* 2008, **47**, 4542. (b) X. Liu, J. Feng, A. Ren, L. Yang, B. Yang and Y. Ma, *Optical Materials,* 2006, **29**, 231. (c) T. Liu, B.-H. Xia, X. Zhou, Q.-C. Zheng, Q.-J. Pan and H.-X. Zhang, *Theor. Chem. Acc.,* 2008, **121**, 155. (d) T. Liu, B.-H. Xia, X. Zhou, H.-X. Zhang, Q.-J. Pan and J.-S. Gao, *Organometallics,* 2007, **26**, 143. (e) X. Gu, T. Fei, H. Zhang, H. Xu, B.Yang, Y. Ma and X. Liu, *J. Phys. Chem. A,* 2008, **112**, 8387. (f) Y. H. Lee, N. G. Park, Y. Ha, Y. S. Kim, *Japanese J. Appl. Phys.,* 2006, **45**, 563. (g) H. J. Bolink, L. Cappelli, S. Cheylan, E. Coronado, R. D. Costa, N. Lardiés, M. K. Nazeeruddin and E. Ortí, *J. Mater. Chem.,* 2007, **17**, 5032. (h) Y. H. Lee and Y. S. Kim, *Curr. Appl. Phys.,* 2007, **7**, 504. (i) X. Gu, T. Fei, H. Zhang, H. Xu, B. Yang, Y. Ma and X. Liu, *Eur. J. Inorg. Chem.,* **2009**, 2407. (j) D. Di Censo, S. Fantacci, F. De Angelis, C. Klein, N. Evans, K. Kalyanasundaram, H. J. Bolink, M. Grätzel and M. K. Nazeeruddin, *Inorg. Chem.,* 2008, **47**, 980. (k) X. Zeng, M. Tavasli, I. F. Perepichka, A. S. Batsanov, M. R. Bryce, C.-J. Chiang, C. Rothe and A. P.Monkman, *Chem. Eur. J.,* 2008, **14**, 933. (l) J. Li, P. I. Djurovich, B. D. Alleyne, M. Yousufuddin, N. N. Ho, J. C. Thomas, J. C. Peters, R. Bau and M. E. Thompson, *Inorg. Chem*., 2005, **44**, 1713. (m) F. De Angelis, S. Fantacci, N. Evans, C. Klein, S. M. Zakeeruddin, J.-E. Moser, K. Kalyanasundaram, H. J. Bolink, M. Grätzel and M. K. Nazeeruddin, *Inorg. Chem.,* 2007, **46**, 5989.

8 D. Nie, Z. Liu, Z. Bian and C. Huang, *J. Mol. Struct. THEOCHEM,* 2008, **861**, 97.

9 X. Li, Q. Zhang, Y. Tu, H. Agren and H. Tian, *Phys. Chem. Chem. Phys.,* 2010, **12**,13730.

10 (a) T. H. Dunning, Jr. and P. J. Hay, in *Modern Theoretical Chemistry*, Editor: Schaefer, H. F. III, Vol. 3, Plenum, New York, 1976, 1-28. (b) P. J. Hay and W. R. Wadt, *J. Chem. Phys.,* 1985, **82**, 270. (c) W. R. Wadt and P. J. Hay, *J. Chem. Phys.,* 1985, **82**, 284. (d) P. J. Hay and W. R. Wadt, *J. Chem. Phys.,* 1985, **82**, 299.

11 (a) G. A. Petersson and M. A. Al-Laham, *J. Chem. Phys.,* 1991, **94**, 6081. (b) G. A. Petersson, A. Bennett, T. G. Tensfeldt, M. A. Al-Laham, W. A. Shirley and J. Mantzaris, *J. Chem. Phys.,* 1988, **89**, 2193.

12 J. P. Perdew, K. Burke and M. Ernzerhof, *Phys. Rev. Lett.,* 1996, **77**, 3865.

13 (a) B. J. Lynch, P. L. Fast, M. Harris and D. G. Truhlar, *J. Phys. Chem., A* 2000, **104**, 4811. (b) B. J. Lynch, Y. Zhao and D. G. Truhlar, *J. Phys. Chem., A* 2003, **107**, 1384.

14 T. Yanai, D. P. Tew and N. C. Handy, *Chem. Phys. Lett.,* 2004, **393**, 51.

15 A. P. Scott and L. Radom, *J. Phys. Chem*., 1996, **100**, 16502.

Electronic Supplementary Material (ESI) for Journal of Materials Chemistry
This journal is © The Royal Society of Chemistry 2012

16 A. E. Aliev, D. Courtier-Murias and S. Zhou, *J. Mol. Struct. THEOCHEM,* 2009, **893**, 1.

17 R. J. F. Berger, H.-G. Stammler, B. Neumann and N. W. Mitzel, *Eur. J. Inorg. Chem.,* **2010**, 1613.

18 A. B. Tamayo, B. D. Alleyne, P. I. Djurovich, S. Lamansky, I. Tsyba, N. N. Ho, R. Bau and M. E. Thompson, *J. Am. Chem. Soc.,* 2003, **125**, 7377.

19 M. Tavasli, S. Bettington, M. R. Bryce, A. S. Batsanov and A. P. Monkman, *Synthesis,* **2005**, 1619.

20 K. Nozaki, *J. Chinese Chem. Soc*., 2006, **53**, 101.

21 E. Jansson, B. Minaev, S. Schrader and H. Ågren, *Chem. Phys*., 2007, **33***,* 157.

22 T. Matsushita, T. Asada and S. Koseki, *J. Phys. Chem. C,* 2007, **111**, 6897.

23 Y. Wu and J.-L. Bredas, *J. Chem. Phys*., 2008, **129**, 214305.

24 A. R. Allouche, *J. Comput. Chem*., 2011, **32**, 174.

25 N. M. O'Boyle, A. L. Tenderholt and K. M. Langner, *J. Comput. Chem*., 2008, **29**, 839.

26 K. Dedeian, P. I. Djurovich, F. O. Garces, G. Carlson and R. J. Watts, *Inorg. Chem.,* 1991, **30**, 1685.